Stabilized extended finite elements for the approximation of saddle point problems with unfitted interfaces

Laura Cattaneo · Luca Formaggia · Guido Francesco Iori · Anna Scotti · Paolo Zunino

Received: 12 July 2013 / Accepted: 14 January 2014 / Published online: 7 February 2014

L. Cattaneo · L. Formaggia · G. F. Iori (✉) · A. Scotti · P. Zunino
MOX, Department of Mathematics, Politecnico di Milano, 20133 Milano, Italy
e-mail: guidofr.iori@gmail.com

P. Zunino
Department of Mechanical Engineering and Materials Science, University of Pittsburgh, Pittsburgh, PA 15261, USA

1 Introduction and problem set up

Extended finite element methods (XFEMs) represent a vivid subject of research in the field of computational mechanics [13,21]. The aim of XFEMs is to enable the accurate approximation of problems whose solutions involve jumps, kinks, singularities and other locally non-smooth features within elements. This is achieved by enriching the polynomial approximation space of the classical finite element method with non-smooth functions that resemble the true solution near interfaces. Such methods have shown their potential in several applications of solid mechanics, such as the finite element analysis of cracks, shear bands, dislocations, solidification, and multi-field problems.

Recently, XFEM has been applied to flow problems with moving interfaces, such as the numerical simulation of flows involving immiscible fluids, see for example [15] for a broad introduction or [23] more specific applications. In this context, different types of enrichment strategies for the finite element approximation spaces have been proposed. The method originally proposed in [16] for the approximation of the Laplace equation with contrast coefficients is particularly effective, see also [1,27], owing to the good approximation properties and the simplicity of implementation. Indeed, it has been successfully extended to the approximation of saddle point problems in [2,3, 8,17]. The main drawback of the method consists in the lack of robustness when the interface cuts the mesh in a way that very small sub-elements are created. Stabilization methods based on the interior penalty approach have been proposed to override this issue [3,9]. As it will be confirmed by the numerical experiments reported below, for saddle point problems additional instabilities arise because the enrichment of the Lagrange multiplier space (the pressure) affects the satisfaction of the *inf-sup* condition [5]. There are two possible solutions of this issue. On one hand, the enrichment method could be modified. This strategy has been investigated in a series of works [2,10,24]. It seems to be a promising method. However, a complete stability analysis of the proposed approximation spaces is not available yet. On the other hand, the stabilization methods developed to cure the instabilities with respect to small cut-elements may also help to stabilize the pressure. This is the approach successfully adopted in [3,17].

We aim to investigate the application of XFEMs, in particular of the method proposed in [16], to the approximation of saddle point problems. This method combines weak enforcement of interface conditions using Nitsche's method with XFEM approximation spaces.

From now on, we will refer to this family of methods as the Nitsche-XFEM schemes, as proposed in [15]. In particular, we focus our attention on Stokes equations and the

related applications. Given a bounded domain $\Omega \subset \mathbb{R}^2$ crossed by an interface Γ dividing Ω into two open sets Ω_1 and Ω_2 we solve:

$$\begin{cases} -\nabla \cdot (\mu_i \nabla \mathbf{u}) + \nabla p = \mathbf{f} & \text{in } \Omega_i, \\ \nabla \cdot \mathbf{u} = 0 & \text{in } \Omega_i, \\ \mathbf{u} = 0 & \text{on } \partial\Omega, \\ [\![\mathbf{u}]\!] = 0 & \text{on } \Gamma, \\ [\![p\mathbf{n} - \mu \nabla \mathbf{u} \cdot \mathbf{n}]\!] = 0 & \text{on } \Gamma. \end{cases} \tag{1}$$

The parameter μ_i plays the role of fluid viscosity and is constant in each subdomain Ω_i. Here, since $\mu_1 \neq \mu_2$, the continuity of stresses across Γ induces a kink on the velocity field and a strong discontinuity on pressure (also called jump discontinuity). This is a consequence of the interface conditions $(1)_{d,e}$ where $[\![v]\!] = v|_{\Omega_1} - v|_{\Omega_2}$ denotes the jump across Γ. Accordingly, $\mathbf{n}$ is the unit normal vector on Γ pointing from Ω_1 to Ω_2. The equilibrium condition between the normal component of the stresses may be generalized to include surface tension as follows:

$$[\![p\mathbf{n} - \mu \nabla \mathbf{u} \cdot \mathbf{n}]\!] = \tau \kappa \mathbf{n} \quad \text{on } \Gamma,$$

where κ is the curvature of Γ and τ is the surface tension coefficient [15]. This more general condition can be naturally embedded into the numerical method that we will develop, giving rise to an additional right hand side proportional to $\tau\kappa\mathbf{n}$. Surface tension introduces a jump discontinuity across the interface in the pressure field, which can be accurately captured by the scheme. As a consequence, most of the results that we will present remain valid when surface tension is accounted for. Only the error analysis (Theorem 2) should be carefully reviewed, because the additional term decreaes the regularity that can be assumed for the exact solution of problem [22].

An approach based on finite elements where the computational mesh does not fit to the interface is not suitable for these kind of problems, because it does not satisfy optimal approximation properties. To preserve accuracy, the strong or weak discontinuities in the solution must coincide with mesh edges. However, for many time-dependent problems such as two-phase flows or fluid-structure interaction, non-matching grid formulations become an interesting option because they avoid remeshing [23,25,26].

Mixed finite elements are a typical choice of approximation spaces for the discrete formulation of a saddle point problem without interface. It would be natural to expect that the same finite element spaces would be adequate to solve the interface problem using the Nitsche-XFEM formulation. The numerical experiment shown in Fig. 1 reveals that XFEM spaces do not inherit the *inf-sup* stability of the underlying FEM approximation. More precisely, Fig. 1 suggests that pressure oscillations, resembling to the checkerboard instability, appear in the neighborhood of the interface. In this case, the Nitsche-XFEM formulation is applied to solve problem (1) on a quasi uniform mesh cut by a circular interface separating two regions characterized by heterogeneous viscosities. Following the approach already adopted in [3,17], we investigate how to avoid these oscillations by the choice of suitable enriched finite element spaces and stabilization terms. However, instead of stabilization techniques based on the interior penalty technique, we study the behavior of the well known Brezzi–Pitkaranta stabi-

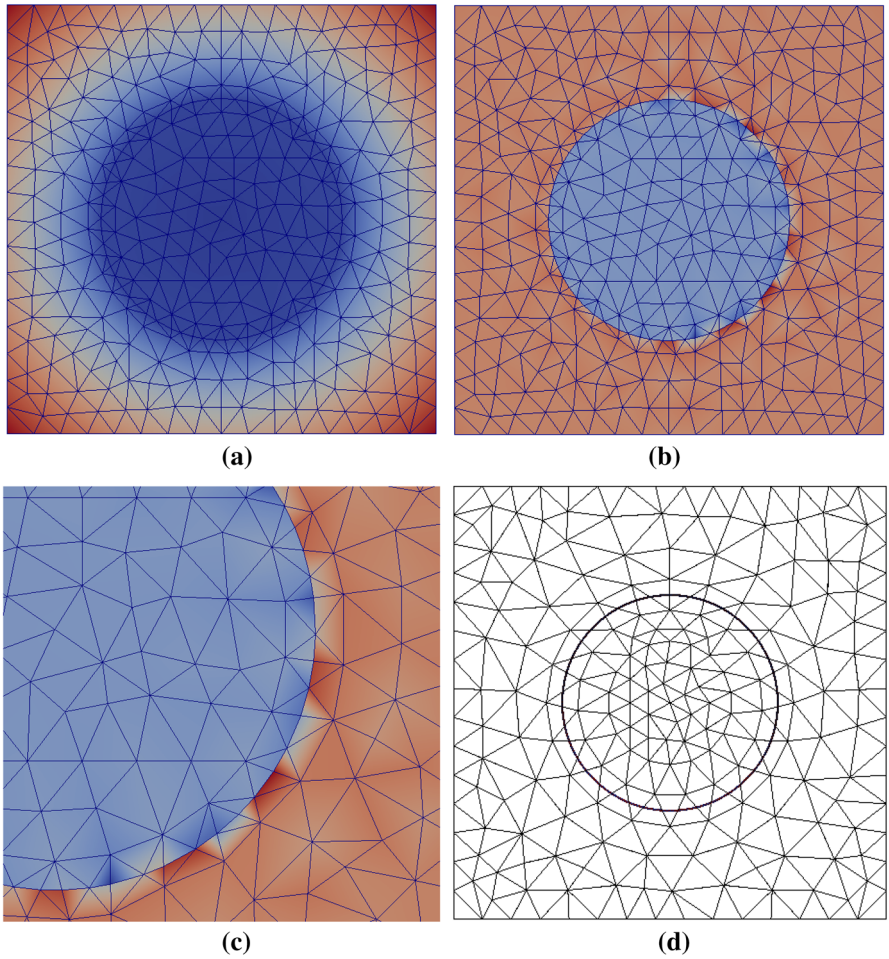

Fig. 1 For the test case #3 reported in Sect. 4, we show the typical checkerboard pattern of instabilities for the pressure in the cut region (**b**), while velocity approximation is not affected by instabilities, as confirmed by the visualization of the velocity field magnitude (**a**). In picture (**c**), a zoom on the pressure instabilities and in picture (**d**) the mesh that has been used for testing the conditioning of the problem, which results are also reported in Sect. 4

lization technique [6] applied to this new context. Finally, we address the properties of the algebraic system of equations arising from the proposed discretization method. In particular, we study the spectrum of the Schur complement matrix, showing that the stabilization method is essential to ensure that the conditioning of the system does not depend on the diameter of cut-elements. This result has an important consequence. It confirms that the classical solution methods for algebraic saddle point problems, such as the Uzawa method, can be successfully combined with this approximation scheme.

A recent result on the stabilization of Stokes problem with interfaces in the context of fictitious domain method has been presented in [19]. Here, pressure is stabilized

by the addition of penalty terms for the jumps in the normal velocity and pressure gradients in the vicinity of the interface.

2 Finite element formulation

We solve (1) on a conforming triangulation $\mathcal{T}_h$ of Ω which is independent of the location of the interface Γ. However, we need to make some assumptions concerning the intersection between Γ and the mesh. Let us define the subset of cut elements $\mathcal{G}_h = \{K \in \mathcal{T}_h \text{ such that } K \cap \Gamma \neq \emptyset\}$, see Fig. 2a. In the following, we call this subset of elements *cut region*. Moreover, let us define the triangulated restricted and extended sub-domains, Ω_i^-, Ω_i^+ respectively, as follows

$$\Omega_i^+ = \{\mathbf{x} \in K, \forall K \text{ such that } K \cap \Omega_i \neq \emptyset\}, \quad \Omega_i^- = \{\mathbf{x} \in K, \forall K \text{ such that } K \subset \Omega_i\}.$$

We observe that $\Omega_i^- \subset \Omega_i^+$ and

$$\Omega = \Omega_1^- \bigcup \Omega_2^- \bigcup \mathcal{G}_h, \quad \Omega_i^+ = \Omega_i^- \bigcup \mathcal{G}_h.$$

We make the following assumptions:

- **Assumption A1** For any element K in the cut region and $i = 1, 2$ there exists a patch formed by the union of the element K with some of the elements of Ω_i^- sharing with it an edge (see Fig. 2a). This collection of elements is called a macro-element of K and it is denoted with $M_{K,i}$. Furthermore, we assume that the restriction of each macro-element to Ω_i^- is not empty, namely $M_{K,i}^- := M_{K,i} \cap \Omega_i^- \neq \emptyset$. Finally, we observe that $M_{K,i}^-$ contains at least one element of $\mathcal{T}_h$, such that the ratio $|M_{K,i}|/|M_{K,i}^-|$ is always upper bounded, where the symbol $|\cdot|$ represents the measure of a subset in $\mathbb{R}^2$.
- **Assumption A2** Γ intersects each element boundary ∂K exactly twice, and each (open) edge at most once, see Fig. 3.
- **Assumption A3** The interface is defined by the zero isoline of a level set function; the level set function is then approximated by linear interpolation on the computational mesh. The interface is thus represented by a chain of straight segments. We assume that the straight line segment $\Gamma_{K,h}$ connecting the points of intersection between Γ and ∂K is a good approximation of $\Gamma_K = \Gamma \cap K$ in a sense that is detailed in [16], Assumption 3. This construction can be generalized to three space dimensions.

The first assumption is satisfied if the mesh is uniform, at least in the region neighboring the interface Γ. The last two hypotheses imply that the discrete approximation of the interface subdivides elements into simple shapes (a triangle and a quadrilateral or a couple of triangles).

We can now define the *extended cut region* $\mathcal{S}_h$ as the union of $\mathcal{G}_h$ and all the elements $K \in \mathcal{T}_h$ sharing an edge with at least one cut element (see Fig. 2b). This is equivalent to define $\mathcal{S}_h$ as the set of all the elements contained in at least one macro-element for all $K \in \mathcal{G}_h$ (Fig. 2):

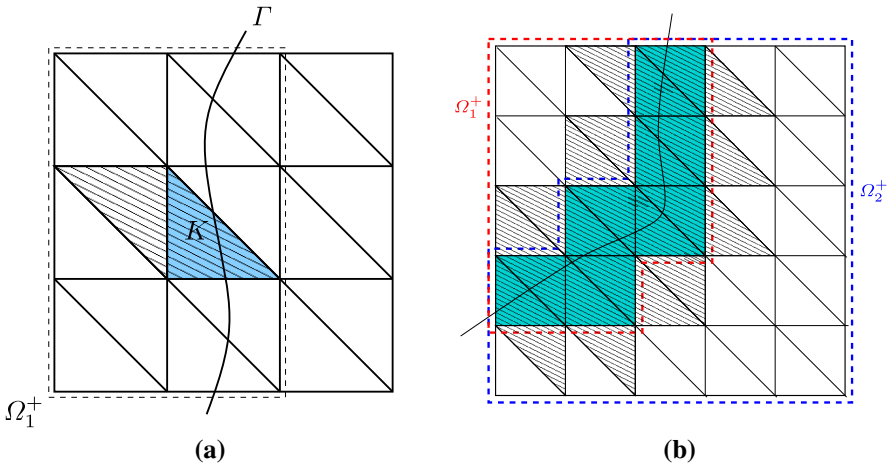

Fig. 2 **a** Filled with the *diagonal line* pattern, a macro-element for an element $K \in \mathcal{G}_h$ (in *light blue*). This macro-pattern is composed by K and its adjacent element that shares an edge with it. **b** Definition of Ω_i^+, in *light blue* the set $\mathcal{G}_h$ and filled with the *diagonal line* pattern the *extended cut region* $\mathcal{S}_h$. As we can see, the extended region contains all the elements near to the cut region, meaning that they share an edge with at least one cut element (color figure online)

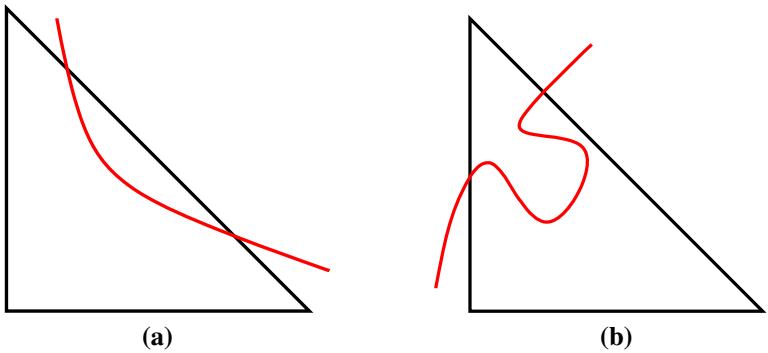

Fig. 3 Second (**a**) and third (**b**) assumption about the intersection between Γ and $\mathcal{T}_h$ are not satisfied

$$\mathcal{S}_h := \bigcup_{K \in \mathcal{G}_h} \bigcup_{i=1,2} M_{K,i}.$$

The proposed XFEM method doubles the degrees of freedom in the elements that are crossed by the discontinuity interface, as shown in Fig. 4. This is achieved by a suitable definition of the approximation spaces. Let $\mathcal{T}_{h,i}^+$ be conforming triangulations of Ω_i^+ such that the union of $\mathcal{T}_{h,1}^+$ and $\mathcal{T}_{h,2}^+$ gives $\mathcal{T}_h$ and for every triangle $K \in \mathcal{T}_{h,1}^+ \cap \mathcal{T}_{h,2}^+$ we have $K \cap \Gamma \neq \emptyset$. Moreover, we define $\mathcal{T}_{h,i}^- = \mathcal{T}_{h,i}^+ \setminus \mathcal{G}_h$.

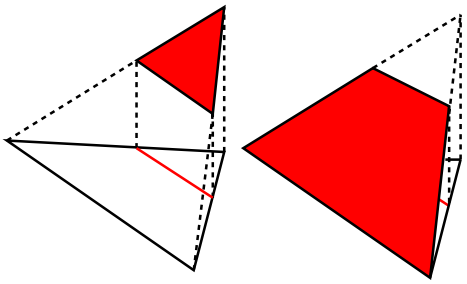

Fig. 4 Linear basis function in an element crossed by Γ. The local basis functions ϕ on a cut element K must be discontinuous across Γ : $\phi = \begin{cases} \phi_1 \text{ in } K_1 = K \cap \Omega_1 \\ \phi_2 \text{ in } K_2 = K \cap \Omega_2 \end{cases}$. Since ϕ_1 and ϕ_2 must be independent, we need to double the degrees of freedom on K so that ϕ_1 can be represented in K_1 by its nodal values and the same holds for ϕ

Let us define the following couple of *inf-sup* stable spaces on Ω,

$$V(\Omega) := [\{\phi_h \in C^0(\Omega), \text{ such that } \phi_h|_K \in \mathbb{P}^1, \forall K \in \mathcal{T}_h\} \cap H_0^1(\Omega) \oplus B]^2,$$
$$Q(\Omega) := \{\phi_h \in C^0(\Omega), \text{ such that } \phi_h|_K \in \mathbb{P}^1, \forall K \in \mathcal{T}_h\},$$

where $B = \{b \text{ such that } b|_K \in \mathbb{P}^3 \cap H_0^1(K), \forall K \in \mathcal{T}_h\}$.
In alternative, we may use the plain $\mathbb{P}^1 - \mathbb{P}^1$ elements,

$$V(\Omega) := [\{\phi_h \in C^0(\Omega), \text{ such that } \phi_h|_K \in \mathbb{P}^1, \forall K \in \mathcal{T}_h\}]^2,$$
$$Q(\Omega) := \{\phi_h \in C^0(\Omega), \text{ such that } \phi_h|_K \in \mathbb{P}^1, \forall K \in \mathcal{T}_h\},$$

that will be combined with a stabilization term defined below. We now introduce the couple of *inf-sup* stable spaces on the restricted sub-domains Ω_i^-,

$$V_{h,i}^- := \{\phi_h \in V(\Omega_i^-), \text{ such that } \phi_h = 0 \text{ on } \Gamma\},$$
$$Q_{h,i}^- := Q(\Omega_i^-).$$

Let $\mathcal{I}_\Gamma = \{1, \ldots, n\}$ be the set of all vertexes in the *cut region* $\mathcal{G}_h$ and let

$$W_h = \{\phi_h \in C^0(\Omega), \text{ such that } \phi_h|_K \in \mathbb{P}^1, \forall K \in \mathcal{T}_h\} \cap H_0^1(\Omega)$$

be a standard linear finite element space on the triangulation $\mathcal{T}_h$ of the domain Ω and let $\{\phi_h^j\}$ be the Lagrangian basis of W_h. We can now define a couple of finite element spaces on the *cut region*:

$$V_h^{cut} := [span\{\phi_h^j \in W_h\}_{j \in \mathcal{I}_\Gamma}]^2, \quad Q_h^{cut} := span\{\phi_h^j \in W_h\}_{j \in \mathcal{I}_\Gamma}.$$

The definition of the finite element spaces for the approximation of (1) follows:

$$V_{h,i} := V_{h,i}^- \oplus V_h^{cut}, \quad Q_{h,i} := Q_{h,i}^- \oplus Q_h^{cut}.$$

The enrichment of the *cut region* is obtained by overlapping the spaces $V_{h,i}$ and $Q_{h,i}$ in $\mathcal{G}_h$ which entails that the degrees of freedom of the elements $K \in \mathcal{G}_h$ are doubled. We seek $(\mathbf{u}_{h,i}, p_{h,i}) \in V_{h,i} \times Q_{h,i}, i = 1, 2$ such that $\mathbf{u}_h = (\mathbf{u}_{h,1}, \mathbf{u}_{h,2})$ and $p_h = (p_{h,1}, p_{h,2})$ satisfy:

$$\mathcal{B}_h[(\mathbf{u}_h, p_h), (\mathbf{v}_h, q_h)] + s_h(p_h, q_h) = (\mathbf{f}, \mathbf{v}_h)_\Omega, \forall (\mathbf{v}_h, q_h) \in V_h \times Q_h, \tag{2}$$

where $V_h = V_{h,1} \times V_{h,2}$, $Q_h = Q_{h,1} \times Q_{h,2}$ and

$$\begin{aligned}
\mathcal{B}_h[(\mathbf{u}_h, p_h), (\mathbf{v}_h, q_h)] &:= a_h(\mathbf{u}_h, \mathbf{v}_h) + b_h(p_h, \mathbf{v}_h) - b_h(q_h, \mathbf{u}_h) \\
a_h(\mathbf{u}_h, \mathbf{v}_h) &:= \sum_{i=1,2} \int_{\Omega_i} \mu_i \nabla \mathbf{u}_{h,i} \cdot \nabla \mathbf{v}_{h,i} dx - \int_\Gamma \{\{\mu \nabla \mathbf{u}_h \cdot \mathbf{n}\}\} [\![\mathbf{v}_h]\!] ds \\
&- \int_\Gamma \{\{\mu \nabla \mathbf{v}_h \cdot \mathbf{n}\}\} [\![\mathbf{u}_h]\!] ds + \sum_{K \in \mathcal{G}_h} \int_{\Gamma_K} \gamma_u h_K^{-1} \mu_{max} [\![\mathbf{u}_h]\!] [\![\mathbf{v}_h]\!] ds \\
b_h(p_h, \mathbf{v}_h) &:= - \sum_{i=1,2} \int_{\Omega_i} p_{h,i} \nabla \cdot \mathbf{v}_{h,i} dx + \int_\Gamma \{\{p_h\}\} [\![\mathbf{v}_h \cdot \mathbf{n}]\!] ds.
\end{aligned}$$

where h_K is the diameter of the generic element K. We fix $\mu_{max} = \max_\Omega \mu$ and we define the average operator as $\{\{v\}\}_\Gamma = k_1 v|_{\Omega_1} + k_2 v|_{\Omega_2}$. For each element $K \in \mathcal{G}_h$, it must hold $k_1 + k_2 = 1$. For this scheme it is important that the weights depend of the measure of cut elements, for example $k_i = |K \cap \Omega_i|/|K|$. In particular, we use the following definition proposed in [1]:

$$k_i := \frac{|K \cap \Omega_i|/\mu_i}{|K \cap \Omega_1|/\mu_1 + |K \cap \Omega_2|/\mu_2}. \tag{3}$$

We remark that in the case $\mu_1 = \mu_2$ the last two definitions coincide.

The term $s_h(p_h, q_h)$ is the stabilization operator defined on the cut region. We are interested in analyzing the properties of the Brezzi–Pitkaranta stabilization technique [6] applied to this new context. For this reason, we consider the following operator acting on the pressure approximation near the interface:

$$s_h(p_h, q_h) := \sum_{i=1,2} \sum_{K \in \mathcal{S}_h} \gamma_s \mu_i^{-1} h_K^2 \int_K \nabla p_{h,i} \cdot \nabla q_{h,i} dx, \tag{4}$$

where $\mathcal{S}_h$ is the *extended cut region* previously defined. We remark that the integral in (4) is on the entire element K. This is crucial to prevent a bad conditioning of the algebraic problem. As we have already pointed out, our choice of spaces $V_{h,i}^-$ and $Q_{h,i}^-$ is *inf-sup* stable on the restricted sub-domains. In the case of equal-order stabilized velocity/pressure formulation we add to the discrete problem formulation the additional stabilization term $c_h(p_h, q_h)$. Although $c_h(p_h, q_h)$ can be chosen among the family of symmetric stabilization operators, the most natural choice in our case is the Brezzi–Pitkaranta stabilization:

$$c_h(p_h, q_h) := \sum_{i=1,2} c_{h,i}(p_h, q_h), \quad \text{where}$$
$$c_{h,i}(p_h, q_h) := \sum_{K \in \mathcal{T}_{h,i}^-} \gamma_s \mu_i^{-1} h_K^2 \int_K \nabla p_{h,i} \cdot \nabla q_{h,i} dx.$$

In this case, we aim to find $\mathbf{u}_h = (\mathbf{u}_{h,1}, \mathbf{u}_{h,2}) \in V_h$ and $p_h = (p_{h,1}, p_{h,2}) \in Q_h$ such that

$$\mathcal{B}_h[(\mathbf{u}_h, p_h), (\mathbf{v}_h, q_h)] + c_h(p_h, q_h) + s_h(p_h, q_h) = (\mathbf{f}, \mathbf{v}_h)_\Omega, \forall (\mathbf{v}_h, q_h) \in V_h \times Q_h. \tag{5}$$

In the forthcoming sections, we will analyze the two proposed variants of the Nitsche-XFEM scheme.

A final remark concerns mass conservation. It is well known that stabilization techniques of Brezzi–Pitkaranta type introduce a consistency error in the mass conservation equation which is, in the classical setting, of order h^2. We wish to point out that in our proposed technique for $\mathbb{P}_b^1 - \mathbb{P}^1$ elements, the stabilization term is activated only in the subset $\mathcal{S}_h$ of elements adjacent to the interface Γ. Since the number of elements in $\mathcal{S}_h$ scales like h^{-1} (and not h^{-2} as the total number of mesh elements), the error in mass conservation introduced by our proposed method is of order h^3. Thus, in our opinion, it is acceptable in practice.

3 Analysis of the scheme

First of all, let us define the following norms on the trace of a function on Γ:

$$\|v\|_{1/2,h,\Gamma}^2 := \sum_{K \in \mathcal{G}_h} h_K^{-1} \|v\|_{0,\Gamma_K}^2, \qquad \|v\|_{-1/2,h,\Gamma}^2 := \sum_{K \in \mathcal{G}_h} h_K \|v\|_{0,\Gamma_K}^2.$$

Then, we introduce the following broken Sobolev spaces: $H_b^k = \{v : v|_{\Omega_i} \in H^k(\Omega_i), i = 1, 2\}$ with the corresponding norms

$$\|\mathbf{v}\|_{k,\Omega}^2 := \sum_{i=1,2} \|\mathbf{v}\|_{k,\Omega_i}^2, \quad \|\mathbf{v}\|_{k,\Omega,\mu}^2 := \sum_{i=1,2} \|\mu_i^{1/2} \mathbf{v}\|_{k,\Omega_i}^2,$$
$$\|q\|_{k,\Omega^\pm,\mu}^2 := \sum_{i=1,2} \|\mu_i^{-1/2} q\|_{k,\Omega_i^\pm}^2,$$
$$|||\mathbf{v}|||^2 := \|\mathbf{v}\|_{1,\Omega,\mu}^2 + \|\mu_{max}^{1/2} [\![\mathbf{v}]\!]\|_{1/2,h,\Gamma}^2 + \|\mu_{max}^{-1/2} \{\!\{\mu \nabla_{\mathbf{n}} \mathbf{v}\}\!\}\|_{-1/2,h,\Gamma}^2,$$
$$\|(\mathbf{v}, q)\|_{\Omega^+}^2 := |||\mathbf{v}|||^2 + \|q\|_{0,\Omega^+,\mu}^2 + \|\mu_{max}^{-1/2} \{\!\{q\}\!\}\|_{-1/2,h,\Gamma}^2.$$

Let us define $b_{h,i}(p_h, q_h)$ as the restrictions of $b_h(p_h, q_h)$ on the domains Ω_i,

$$b_{h,i}(p_h, q_h) := -\int_{\Omega_i} p_{h,i} \nabla \cdot \mathbf{v}_{h,i} dx,$$

and let us introduce the discrete trace inequality

$$h_K \|v\|^2_{0,\Gamma_K} \leq C \|v\|^2_{0,K}, \tag{6}$$

which will be necessary for the theoretical analysis, as in [17], and proved thanks to [4] and [16]. Thanks to this inequality, taking $q_h \in Q_h$, we have,

$$\begin{aligned}
\|\mu_{max}^{-1/2} \{\{q\}\}\|^2_{-1/2,h,\Gamma} &\leq \|\left\{\left\{\mu^{-1/2} q_h\right\}\right\}\|^2_{-1/2,h,\Gamma} = \sum_{K\in\mathcal{G}_h} h_K \|\left\{\left\{\mu^{-1/2} q_h\right\}\right\}\|^2_{0,\Gamma_K} \\
&\leq \sum_{K\in\mathcal{G}_h} h_K \left(\|\mu_1^{-1/2} k_1 q_{h,1}\|^2_{0,\Gamma_K} + \|\mu_2^{-1/2} k_2 q_{h,2}\|^2_{0,\Gamma_K}\right) \\
&\leq C \sum_{i=1,2} \sum_{K\in\mathcal{G}_h} \|\mu_i^{-1/2} k_i q_{h,i}\|^2_{0,K} \\
&\leq C \sum_{i=1,2} \sum_{K\in\mathcal{G}_h} \|\mu_i^{-1/2} q_{h,i}\|^2_{0,K} \\
&\leq C \sum_{i=1,2} \sum_{K\in\mathcal{T}^+_{h,i}} \|\mu_i^{-1/2} q_{h,i}\|^2_{0,K} = C \|q_h\|^2_{0,\Omega^+,\mu}.
\end{aligned}$$

In particular, the following equivalence of discrete norms holds true,

$$|||\mathbf{v}|||^2 + \|q_h\|^2_{0,\Omega^+,\mu} \leq \|(\mathbf{v}, q_h)\|^2_{\Omega^+} \leq |||\mathbf{v}|||^2 + (1+C)\|q_h\|^2_{0,\Omega^+,\mu}. \tag{7}$$

3.1 Stability analysis

The first part of our theoretical analysis focuses on the stability of the scheme.

Theorem 1 *We assume that there exist constants C_{p1} and C_{p2}, independent of the mesh size, such that $\forall p_{h,i} \in Q_{h,i}$ there exists $\mathbf{v}_{p_{h,i}} \in V_{h,i} : \mathbf{v}_{p_{h,i}}|_{\mathcal{G}_h} = 0$ such that*

$$\|\mathbf{v}_{p_{h,i}}\|_{1,\Omega_i^-,\mu} \leq C_{p1} \|p_{h,i}\|_{0,\Omega_i^-,\mu}, \tag{8}$$

$$C_{p2} \|p_{h,i}\|_{0,\Omega_i^-,\mu} \leq b_{h,i}(p_{h,i}, \mathbf{v}_{p_{h,i}}) + c_{h,i}(p_{h,i}, p_{h,i}). \tag{9}$$

These are sufficient conditions for the stability of the approximation on the subregion Ω_i^-, see [12]. Under this assumption, there exists a positive constant C_s, independent of the mesh characteristic size such that, for any $(\mathbf{u}_h, p_h) \in V_h \times Q_h$ it holds:

$$C_s \|(\mathbf{u}_h, p_h)\|_{\Omega^+} \leq \sup_{(\mathbf{v}_h, q_h)\in V_h\times Q_h} \frac{\mathcal{B}_h[(\mathbf{u}_h, p_h), (\mathbf{v}_h, q_h)] + c_h(p_h, q_h) + s_h(p_h, q_h)}{\|(\mathbf{v}_h, q_h)\|_{\Omega^+}}. \tag{10}$$

We remark that (8) implies

$$\|\mathbf{v}_{p_{h,i}}\|_{1,\Omega_i^-,\mu} \leq C_{p1} \|p_{h,i}\|_{0,\Omega_i^+,\mu}.$$

To prove (10), we start showing some properties of the bilinear forms $a_h(\mathbf{u}_h, \mathbf{v}_h)$, $b_h(\mathbf{v}_h, p_h)$, $c_h(p_h, q_h)$ and $s_h(p_h, q_h)$.

Lemma 1 *The bilinear discrete form $a_h(\mathbf{u}_h, \mathbf{v}_h)$ is continuous on V_h and coercive, provided γ_u is chosen sufficiently large. That is, there exist two constants C_m and C_a, independent of the mesh size such that*

$$a_h(\mathbf{u}_h, \mathbf{v}_h) \leq C_m |||\mathbf{u}_h||| \, |||\mathbf{v}_h|||, \quad \forall \mathbf{v}_h \in V_h, \tag{11}$$
$$a_h(\mathbf{v}_h, \mathbf{v}_h) \geq C_a |||\mathbf{v}_h|||^2, \quad \forall \mathbf{v}_h \in V_h. \tag{12}$$

Let $\mathbf{v}_h \in V_h$, $p_h \in Q_h$ and $q_h \in Q_h$. There exist three constants C_b, C_{s1} and C_{s2}, independent of the mesh size, such that

$$b_h(\mathbf{v}_h, p_h) \leq C_b |||\mathbf{v}_h|||(\|p_h\|_{0,\Omega^+,\mu} + \|\mu_{max}^{-1/2} \{\{p_h\}\}\|_{-1/2,h,\Gamma}), \tag{13}$$
$$c_h(p_h, q_h) \leq C_{s1} \|p_h\|_{0,\Omega^+,\mu} \|q_h\|_{0,\Omega^+,\mu}, \tag{14}$$
$$s_h(p_h, q_h) \leq C_{s2} \|p_h\|_{0,\Omega^+,\mu} \|q_h\|_{0,\Omega^+,\mu}. \tag{15}$$

Furthermore, owing to (11) and (13), the bilinear discrete form $\mathcal{B}_h[(\mathbf{u}_h, p_h), (\mathbf{v}_h, q_h)]$ is continuous on $V_h \times Q_h$,

$$\mathcal{B}_h[(\mathbf{u}_h, p_h), (\mathbf{v}_h, q_h)] \leq C_B \|(\mathbf{u}_h, p_h)\|_{\Omega^+} \|(\mathbf{v}_h, q_h)\|_{\Omega^+}. \tag{16}$$

Proof To prove (11), we first prove the following generalized inverse estimate,

$$\|\{\{\mu \nabla_{\mathbf{n}} \mathbf{v}_h\}\}\|^2_{-1/2,h,\Gamma} \leq C_I \mu_{max} \|\mathbf{v}_h\|^2_{1,\Omega,\mu}, \tag{17}$$

where $\nabla_{\mathbf{n}} \mathbf{v}_h = (\nabla \mathbf{v}_h)\mathbf{n}$. This estimate holds true when linear finite elements and the weights k_i defined in (3) are used. In this particular case the constant C_I is such that $C_I \leq 2$. For the proof of (17) we observe that, since $\mathbf{v}_h$ is linear in $\mathcal{G}_h$, for every $K \in \mathcal{G}_h$ we have,

$$\begin{aligned}
\|\{\{\mu \nabla_{\mathbf{n}} \mathbf{v}_h\}\}\|^2_{-1/2,h,\Gamma_K} &= h_K |\Gamma_K| \left(k_1 \mu_1 \nabla_{\mathbf{n}} \mathbf{v}_{h,1} + k_2 \mu_2 \nabla_{\mathbf{n}} \mathbf{v}_{h,2}\right)^2 \\
&\leq h_K \sum_{i=1,2} \frac{|\Gamma_K|}{|K \cap \Omega_i|} k_i^2 \mu_i^2 \|\nabla \mathbf{v}_{h,i}\|^2_{0,K\cap\Omega_i} \\
&= h_K \sum_{i=1,2} \frac{|\Gamma_K|}{|K \cap \Omega_i|} \frac{|K \cap \Omega_i|^2/\mu_i^2}{\left(\sum_{j=1,2} |K \cap \Omega_j|/\mu_j\right)^2} \mu_i^2 \|\nabla \mathbf{v}_{h,i}\|^2_{0,K\cap\Omega_i} \\
&= h_K |\Gamma_K| \frac{1}{\left(\sum_{j=1,2} |K \cap \Omega_j|/\mu_j\right)^2} \sum_{i=1,2} \frac{|K \cap \Omega_i|}{\mu_i} \|\mu_i^{1/2} \nabla \mathbf{v}_{h,i}\|^2_{0,K\cap\Omega_i} \\
&\leq h_K |\Gamma_K| \frac{1}{|K \cap \Omega_1|/\mu_1 + |K \cap \Omega_2|/\mu_2} \sum_{i=1,2} \|\nabla \mathbf{v}_{h,i}\|^2_{0,K\cap\Omega_i,\mu}
\end{aligned}$$

$$\leq \frac{h_K|\Gamma_K|}{|K|}\mu_{max}\|\nabla \mathbf{v}_h\|^2_{0,K,\mu}$$
$$= C_{I,K}\mu_{max}\|\nabla \mathbf{v}_h\|^2_{0,K,\mu}.$$

We point out that, under the assumption of shape-regular mesh, the constant $C_{I,K}$ is bounded independently of the mesh size and the location of the interface Γ. Indeed it is simple to prove that $C_{I,K} \leq 2$.

Summing over all the elements K $\in \mathcal{G}_h$ and setting $C_I = \max_K C_{I,K} \leq 2$ we have

$$\begin{aligned}\|\{\{\mu\nabla_{\mathbf{n}}\mathbf{v}_h\}\}\|^2_{-1/2,h,\Gamma} &\leq \sum_{K\in\mathcal{G}_h} C_{I,K}\mu_{max}\|\nabla \mathbf{v}_h\|^2_{0,K,\mu}\\ &\leq C_I\mu_{max}\sum_{K\in\mathcal{T}_h}\|\nabla \mathbf{v}_h\|^2_{0,K,\mu}\\ &= C_I\mu_{max}\|\nabla \mathbf{v}_h\|^2_{0,\Omega,\mu}.\end{aligned}$$

We are now ready to prove coercivity.

$$\begin{aligned}a_h(\mathbf{v}_h,\mathbf{v}_h) &= \sum_{i=1,2}\int_\Omega \mu_i(\nabla \mathbf{v}_{h,i})^2 dx - 2\int_\Gamma [\![\mathbf{v}_h]\!]\,\{\{\mu\nabla_{\mathbf{n}}\mathbf{v}_h\}\}\,ds\\ &+\int_\Gamma \gamma_u\mu_{max}h_K^{-1}([\![\mathbf{v}_h]\!])^2 ds \geq \|\mathbf{v}_h\|^2_{1,\Omega,\mu} + \gamma_u\|\mu^{1/2}_{max}[\![\mathbf{v}_h]\!]\|^2_{1/2,h,\Gamma}\\ &-2\|\mu^{1/2}_{max}[\![\mathbf{v}_h]\!]\|_{1/2,h,\Gamma}\|\mu^{-1/2}_{max}\{\{\mu\nabla_{\mathbf{n}}\mathbf{v}_h\}\}\|_{-1/2,h,\Gamma}\\ &\geq \|\mathbf{v}_h\|^2_{1,\Omega,\mu} + (\gamma_u-\epsilon)\|\mu^{1/2}_{max}[\![\mathbf{v}_h]\!]\|^2_{1/2,h,\Gamma} - \frac{1}{\epsilon}\|\mu^{-1/2}_{max}\{\{\mu\nabla_{\mathbf{n}}\mathbf{v}_h\}\}\|^2_{-1/2,h,\Gamma}.\end{aligned}$$

Then, it follows form (17) that

$$\begin{aligned}a_h(\mathbf{v}_h,\mathbf{v}_h) &\geq \frac{1}{2}\|\mathbf{v}_h\|^2_{1,\Omega,\mu} + \left(\frac{1}{2}-\frac{2C_I}{\epsilon}\right)\|\mathbf{v}_h\|^2_{1,\Omega,\mu}\\ &+\frac{1}{\epsilon}\|\mu^{-1/2}_{max}\{\{\mu\nabla_{\mathbf{n}}\mathbf{v}_h\}\}\|^2_{-1/2,h,\Gamma} + (\gamma_u-\epsilon)\|\mu^{1/2}_{max}[\![\mathbf{v}_h]\!]\|^2_{1/2,h,\Gamma}.\end{aligned}$$

Taking $\epsilon = 4C_I$ and choosing $\gamma_u > 4C_I$ the coercivity of $a_h(\mathbf{u}_h,\mathbf{v}_h)$ follows, since

$$\begin{aligned}a_h(\mathbf{v}_h,\mathbf{v}_h) \geq \min\left\{\frac{1}{2}, C_{\gamma_u}, \frac{1}{4C_I}\right\}&(\|\mathbf{v}_h\|^2_{1,\Omega,\mu}\\ &+\|\mu^{1/2}_{max}[\![\mathbf{v}_h]\!]\|^2_{1/2,h,\Gamma} + \|\mu^{-1/2}_{max}\{\{\mu\nabla_{\mathbf{n}}\mathbf{v}_h\}\}\|^2_{-1/2,h,\Gamma}),\end{aligned}$$

where $C_{\gamma_u} = (\gamma_u - 4C_I)$. This completes the proof. Continuity of the discrete form $a_h(\mathbf{u}_h,\mathbf{v}_h)$ follows directly from its definition, while to prove the continuity of $b_h(p_h,\mathbf{v}_h)$ we proceed as follows,

$$
\begin{aligned}
b_h(p_h, \mathbf{v}_h) &= -\sum_{i=1,2} \int_{\Omega_i} p_{h,i} \nabla \cdot \mathbf{v}_{h,i} dx + \int_{\Gamma} \{\!\{p_h\}\!\} [\![\mathbf{v}_h \cdot \mathbf{n}]\!] ds \\
&\leq \|p_h\|_{0,\Omega^+,\mu} \|v_h\|_{1,\Omega,\mu} + \|\mu_{max}^{-1/2} \{\!\{p_h\}\!\}\|_{-1/2,h,\Gamma} \|\mu_{max}^{1/2} [\![\mathbf{v}_h \cdot \mathbf{n}]\!]\|_{1/2,h,\Gamma} \\
&\leq C_b |||\mathbf{v}_h||| (\|p_h\|_{0,\Omega^+,\mu} + \|\mu_{max}^{-1/2} \{\!\{p_h\}\!\}\|_{-1/2,h,\Gamma}).
\end{aligned}
$$

Continuity of the stabilization operator $c_h(p_h, q_h)$ is proved as follows,

$$
\begin{aligned}
c_h(p_h, q_h) &= \sum_{i=1,2} \sum_{K \in \mathcal{T}_{h,i}^-} \gamma_s \mu_i^{-1} h_K^2 \int_K \nabla p_{h,i} \cdot \nabla q_{h,i} dx \\
&\leq \sum_{i=1,2} \sum_{K \in \mathcal{T}_{h,i}^-} \gamma_s h_K^2 h_K^{-2} \|\mu_i^{-1/2} p_h\|_{0,K} \|\mu_i^{-1/2} q_h\|_{0,K} \\
&\leq C_{s1} \|p_h\|_{0,\Omega^+,\mu} \|q_h\|_{0,\Omega^+,\mu}.
\end{aligned}
$$

Here the first inequality follows from the inverse inequality. The continuity of $s_h(p_h, q_h)$ is actually obtained in the same way. Summing estimates (11) and (13) and using the definition of the norm $\|(\cdot,\cdot)\|_{\Omega^+}$ yield the result (16). □

To prove the *inf-sup* condition, we first consider a stability estimate for a projection operator.

Lemma 2 *The L^2 projection operator on a macro-element $M_{K,i}$, namely $\Pi_h : H^1(M_{K,i}) \mapsto \mathbb{P}^1(M_{K,i})$, satisfies the following property:*

$$
\|p_{h,i}\|_{0,\Omega_i^+,\mu}^2 \leq C \left(\|p_{h,i}\|_{0,\Omega_i^-,\mu}^2 + \gamma_{h,i}(p_{h,i}, p_{h,i}) \right), \tag{18}
$$

where

$$
\begin{aligned}
\gamma_{h,i}(p_{h,i}, q_{h,i}) &:= \sum_{K \in \mathcal{G}_h} \int_{M_{K,i}} \gamma_s \mu_i^{-1} (1 - \Pi_h) p_{h,i} (1 - \Pi_h) q_{h,i}, \\
\gamma_h(p_h, q_h) &:= \sum_{i=1,2} \gamma_{h,i}(p_{h,i}, q_{h,i})
\end{aligned}
$$

and C is a constant dependent on the total number of elements that can form a macro-element $M_{K,i}$ with a generic element $K \in \mathcal{G}_h$.

Proof Since $\Pi_h p_{h,i}$ is a linear function on a macro-element, it holds that:

$$
\|\Pi_h p_{h,i}\|_{0,M_{K,i}}^2 \lesssim \frac{|M_{K,i}|}{|M_{K,i}^-|} \|\Pi_h p_{h,i}\|_{0,M_{K,i}^-}^2,
$$

where we have introduced the notation $x \lesssim y$ to represent the existence of a generic constant c such that $x \leq cy$. We represent $p_{h,i}|_{M_{K,i}}$ as the sum of the linear part and a residual: $p_{h,i}|_{M_{K,i}} = \Pi_h p_{h,i} + r_{h,i}$. It follows that

$$\begin{aligned}\|p_{h,i}\|^2_{0,M_{K,i}} &= \|\Pi_h p_{h,i} + r_{h,i}\|^2_{0,M_{K,i}} \\ &= \|\Pi_h p_{h,i}\|^2_{0,M_{K,i}} + \|r_{h,i}\|^2_{0,M_{K,i}} \\ &\lesssim \frac{|M_{K,i}|}{|M^-_{K,i}|}\|\Pi_h p_{h,i}\|^2_{0,M^-_{K,i}} + \|r_{h,i}\|^2_{0,M_{K,i}}.\end{aligned}$$

Owing to Assumption A1, the ratio between the measure of the entire macro-element and that of its restriction is upper bounded. We now consider the second member of the last inequality, where we identify $\beta = |M_{K,i}|/|M^-_{K,i}|$ in order to simplify the notation:

$$\begin{aligned}&\beta\|\Pi_h p_{h,i}\|^2_{0,M^-_{K,i}} + \|r_{h,i}\|^2_{0,M_{K,i}} \\ &\quad= \beta\|\Pi_h p_{h,i}\|^2_{0,M^-_{K,i}} - \beta\|r_{h,i}\|^2_{0,M_{K,i}} + (1+\beta)\|r_{h,i}\|^2_{0,M^-_{K,i}} \\ &\quad\le \beta\int_{M^-_{K,i}} (\Pi_h p_{h,i} - r_{h,i})(\Pi_h p_{h,i} + r_{h,i}) + (1+\beta)\|r_{h,i}\|^2_{0,M_{K,i}} \\ &\quad\le \frac{\beta\epsilon}{2}\|\Pi_h p_{h,i} - r_{h,i}\|^2_{0,M_{K,i}} + \frac{\beta}{2\epsilon}\|p_{h,i}\|^2_{0,M^-_{K,i}} + (1+\beta)\|r_{h,i}\|^2_{0,M_{K,i}} \\ &\quad\le \frac{\beta\epsilon}{2}\|\Pi_h p_{h,i}\|^2_{0,M_{K,i}} + \frac{\beta\epsilon}{2}\|r_{h,i}\|^2_{0,M_{K,i}} + \frac{\beta}{2\epsilon}\|p_{h,i}\|^2_{0,M^-_{K,i}} \\ &\qquad+(1+\beta)\|r_{h,i}\|^2_{0,M_{K,i}}.\end{aligned}$$

Since

$$\|p_{h,i}\|^2_{0,M_{K,i}} = \left(1 - \frac{\beta\epsilon}{2}\right)\|p_{h,i}\|^2_{0,M_{K,i}} + \frac{\beta\epsilon}{2}\|\Pi_h p_{h,i}\|^2_{0,M_{K,i}} + \frac{\beta\epsilon}{2}\|r_{h,i}\|^2_{0,M_{K,i}},$$

we obtain

$$\begin{aligned}&\left(1 - \frac{\beta\epsilon}{2}\right)\|p_{h,i}\|^2_{0,M_{K,i}} + \frac{\beta\epsilon}{2}\|\Pi_h p_{h,i}\|^2_{0,M_{K,i}} + \frac{\beta\epsilon}{2}\|r_{h,i}\|^2_{0,M_{K,i}} \\ &\quad\lesssim \frac{\beta\epsilon}{2}\|\Pi_h p_{h,i}\|^2_{0,M_{K,i}} + \frac{\beta\epsilon}{2}\|r_{h,i}\|^2_{0,M_{K,i}} + \frac{\beta}{2\epsilon}\|p_{h,i}\|^2_{0,M^-_{K,i}} + (1+\beta)\|r_{h,i}\|^2_{0,M_{K,i}},\end{aligned}$$

from which it follows that

$$\|p_{h,i}\|^2_{0,M_{K,i}} \lesssim \frac{2\beta}{2\epsilon(2-\beta\epsilon)}\|p_{h,i}\|^2_{0,M^-_{K,i}} + \frac{2(1+\beta)}{2-\beta\epsilon}\|r_{h,i}\|^2_{0,M_{K,i}}. \tag{19}$$

Choosing a suitable ϵ, for instance $\epsilon = \beta^{-1}$ we have

$$\|p_{h,i}\|^2_{0,M_{K,i}} \lesssim \|p_{h,i}\|^2_{0,M^-_{K,i}} + \|r_{h,i}\|^2_{0,M_{K,i}},$$

and, because of the equivalence of the discrete norms,

$$\|\mu^{-1/2} p_{h,i}\|^2_{0,M_{K,i}} \lesssim \|\mu^{-/2} p_{h,i}\|^2_{0,M^-_{K,i}} + \|\mu^{-1/2} r_{h,i}\|^2_{0,M_{K,i}}.$$

To conclude, we sum over all elements of Ω_i^+ and rescale all norms using $\mu_i^{-1/2}$, to obtain

$$\begin{aligned}
\|p_{h,i}\|^2_{0,\Omega_i^+,\mu} &= \|p_{h,i}\|^2_{0,\Omega_i^-,\mu} + \sum_{K\in\mathcal{G}_h} \|\mu_i^{-1/2} p_{h,i}\|^2_{0,K} \\
&\leq \|p_{h,i}\|^2_{0,\Omega_i^-,\mu} + \sum_{K\in\mathcal{G}_h} \|\mu_i^{-1/2} p_{h,i}\|^2_{0,M_{K,i}} \\
&\lesssim \|p_{h,i}\|^2_{0,\Omega_i^-,\mu} + \sum_{K\in\mathcal{G}_h} \left(\|\mu_i^{-1/2} p_{h,i}\|^2_{0,M^-_{K,i}} + \|\mu_i^{-1/2} r_{h,i}\|^2_{0,M_{K,i}} \right) \\
&\lesssim C(\mathcal{T}_h) \left(\|p_{h,i}\|^2_{0,\Omega_i^-,\mu} + \gamma_{h,i}(p_{h,i}, p_{h,i}) \right).
\end{aligned}$$

We remark that, since we sum on the macro-elements of all $K \in \mathcal{G}_h$, some elements will be counted more than once. The mesh-dependent constant $C(\mathcal{T}_h)$ that appear in the proof takes into account this fact. □

This result gives origin to several families of stabilization methods. Notably, the ghost penalty methods as well as the Brezzi–Pitkaranta stabilization can be seen as schemes to control the local operator.

Lemma 3 *The stabilization term*

$$s_h(p_h, q_h) = \sum_{i=1,2} \sum_{K\in\mathcal{S}_h} \gamma_s \mu_i^{-1} h_K^2 \int_K \nabla p_{h,i} \cdot \nabla q_{h,i} dx$$

dominates on the local projection stabilization, that is

$$\gamma_h(q_h, q_h) \lesssim s_h(q_h, q_h). \tag{20}$$

Proof We use the following result [7,12]:

$$\|q_{h,i} - \Pi_h q_{h,i}\|_{0,M_{K,i}} \leq Ch \|\nabla q_{h,i}\|_{L^2(M_{K,i})}, \quad \forall q_{h,i} \in Q_{h,i},$$

where the constant C is independent of the mesh size. We can now write,

$$\begin{aligned}\gamma_h(q_h, q_h) &= \sum_{i=1,2} \sum_{K\in\mathcal{G}_h} \gamma_s \mu_i^{-1} \|(1-\Pi_h) q_{h,i}\|^2_{0,M_{K,i}} \\ &\leq \sum_{i=1,2} \sum_{K\in\mathcal{G}_h} C\gamma_s \mu_i^{-1} h_K^2 \|\nabla q_{h,i}\|^2_{0,M_{K,i}} \\ &\leq C(\mathcal{T}_h) \sum_{i=1,2} \sum_{K\in\mathcal{S}_h} \gamma_s \mu_i^{-1} h_K^2 \|\nabla q_{h,i}\|^2_{0,K} \\ &\lesssim s_h(q_h, q_h).\end{aligned}$$

where $C(\mathcal{T}_h)$ depends on the number of elements that form each macro-element. □

The following property is a consequence of Lemmas 2 and 3:

$$\|p_{h,i}\|^2_{0,\Omega_i^+,\mu} \lesssim \|p_{h,i}\|^2_{0,\Omega_i^-,\mu} + s_h(p_{h,i}, p_{h,i}). \tag{21}$$

It shows that in the Nitsche-XFEM method the discrete pressure can be controlled provided that an inf-sup stable velocity/pressure approximation is combined with the Brezzi–Pitkaranta operator restricted to the neighborhood of the cut region. Using standard arguments, see [3], we now prove that the scheme is stable in the sense specified in Theorem 1.

Proof of Theorem 1 As a first step, we prove the *inf-sup* stability on the domain Ω, given the local stability estimates (on the restricted sub-domains):

$$b(p_h, \mathbf{v}_{p_h}) + c_h(p_h, p_h) + s_h(p_h, p_h) \gtrsim C_{p2} \|p_h\|^2_{0,\Omega^+,\mu}. \tag{22}$$

We take a $\mathbf{v}_{p_h} = (\mathbf{v}_{p_{h,1}}, \mathbf{v}_{p_{h,2}})$ satisfying the assumptions of the theorem and, reminding that $\mathbf{v}_{p_{h,i}}$ are null on the *cut region* since their support is limited to the restricted sub-domain Ω_i^-, we can write:

$$\begin{aligned}b(p_h, \mathbf{v}_{p_h}) &= -\sum_{i=1,2} \int_{\Omega_i} p_{h,i} \nabla\cdot \mathbf{v}_{p_{h,i}} dx + \int_\Gamma \{\{p_h\}\} [\![\mathbf{v}_{p_h}\cdot\mathbf{n}]\!] ds = \sum_{i=1,2} b_{h,i}(p_{h,i}, \mathbf{v}_{p_{h,i}}) \\ &\sum_{i=1,2} \left(b_{h,i}(p_{h,i}, \mathbf{v}_{p_{h,i}}) + c_{h,i}(p_{h,i}, q_{h,i})\right) = b_h(p_h, \mathbf{v}_{p_h}) + c_h(p_h, p_h) \\ &\gtrsim \sum_{i=1,2} C_{p2} \|p_{h,i}\|_{0,\Omega_i^-,\mu}.\end{aligned}$$

Using inequality (21), we are now able to prove the global *inf-sup* stability (22):

$$\begin{aligned}b_h(p_h, \mathbf{v}_{p_h}) + c_h(p_h, p_h) + s_h(p_h, p_h) &\geq \sum_{i=1,2} C_{p2} \|p_{h,i}\|_{0,\Omega_i^-,\mu} + s_h(p_h, p_h) \\ &\gtrsim C_{p2} \|p_h\|^2_{0,\Omega^+,\mu}.\end{aligned}$$

We are now ready to complete the proof. Using the test functions $\mathbf{v}_h = \mathbf{u}_h + \eta \mathbf{v}_{p_h}$ and $q_h = p_h$, we obtain that

$$\begin{aligned}\|(\mathbf{v}_h, q_h)\|_{\Omega^+} &= \|(\mathbf{u}_h + \eta \mathbf{v}_{p_h}, p_h)\|_{\Omega^+} \leq \|(\mathbf{u}_h, p_h)\|_{\Omega^+} + \|(\eta \mathbf{v}_{p_h}, 0)\|_{\Omega^+} \\ &= \|(\mathbf{u}_h, p_h)\|_{\Omega^+} + |||\eta \mathbf{v}_{p_h}||| = \|(\mathbf{u}_h, p_h)\|_{\Omega^+} + \|\eta \mathbf{v}_{p_h}\|_{1,\Omega,\mu}\end{aligned}$$

and using (8) we get,

$$\begin{aligned}\|\eta \mathbf{v}_{p_h}\|^2_{1,\Omega,\mu} &= \eta^2 \|\mathbf{v}_{p_h}\|^2_{1,\Omega,\mu} \leq \eta^2 \sum_{i=1,2} C^2_{p1} \|p_{h,i}\|^2_{0,\Omega_i^-,\mu} \\ &\leq \eta^2 \sum_{i=1,2} C^2_{p1} \|p_{h,i}\|^2_{0,\Omega_i^+,\mu} \leq \eta^2 C^2_{p1} \|(\mathbf{u}_h, p_h)\|^2_{\Omega^+},\end{aligned}$$

which allows us to write,

$$\begin{aligned}\|(\mathbf{v}_h, q_h)\|_{\Omega^+} &\leq \|(\mathbf{u}_h, p_h)\|_{\Omega^+} + \eta C_{p1} \|(\mathbf{u}_h, p_h)\|_{\Omega^+} \\ &= (1 + \eta C_{p1}) \|(\mathbf{u}_h, p_h)\|_{\Omega^+} \lesssim \|(\mathbf{u}_h, p_h)\|_{\Omega^+}.\end{aligned}$$

Now we develop the term $\mathcal{B}_h[(\mathbf{u}_h, p_h), (\mathbf{v}_h, q_h)]$ as

$$\begin{aligned}\mathcal{B}_h[(\mathbf{u}_h, p_h), (\mathbf{v}_h, q_h)] &= a_h(\mathbf{u}_h, \mathbf{u}_h + \eta \mathbf{v}_{p_h}) + b_h(p_h, \mathbf{u}_h + \eta \mathbf{v}_{p_h}) - b_h(p_h, \mathbf{u}_h) \\ &= a_h(\mathbf{u}_h, \mathbf{u}_h) + a_h(\mathbf{u}_h, \eta \mathbf{v}_{p_h}) + b_h(p_h, \eta \mathbf{v}_{p_h}). \qquad (23)\end{aligned}$$

As for the term $a_h(\mathbf{u}_h, \eta \mathbf{v}_{p_h})$, we get

$$\begin{aligned}a_h(\mathbf{u}_h, \eta \mathbf{v}_{p_h}) &= \sum_{i=1,2} \int_{\Omega_i} \mu_i \nabla \mathbf{u}_{h,i} \eta \nabla \mathbf{v}_{p_{h,i}} dx - \int_\Gamma \{\{\mu \eta \nabla_{\mathbf{n}} \mathbf{v}_{p_h}\}\} [\![\mathbf{u}_h]\!] ds \\ &\leq \|\mathbf{u}_h\|_{1,\Omega,\mu} \|\eta \mathbf{v}_{p_h}\|_{1,\Omega,\mu} + \|\mu^{-1/2}_{max} \{\{\mu \eta \nabla_{\mathbf{n}} \mathbf{v}_{p_h}\}\}\|_{-1/2,h,\Gamma} \|\mu^{1/2}_{max} [\![\mathbf{u}_h]\!]\|_{1/2,h,\Gamma} \\ &\leq \frac{\epsilon}{2} \|\mathbf{u}_h\|^2_{1,\Omega,\mu} + \frac{1}{2\epsilon} \|\eta \mathbf{v}_{p_h}\|^2_{1,\Omega,\mu} \\ &\quad + \frac{1}{2\epsilon} \|\mu^{-1/2}_{max} \{\{\mu \eta \nabla_{\mathbf{n}} \mathbf{v}_{p_h}\}\}\|^2_{-1/2,h,\Gamma} + \frac{\epsilon}{2} \|\mu^{1/2}_{max} [\![\mathbf{u}_h]\!]\|^2_{1/2,h,\Gamma}.\end{aligned}$$

Exploiting the trace inequality (17), we get:

$$\begin{aligned}a_h(\mathbf{u}_h, \eta \mathbf{v}_{p_h}) &\leq \frac{\epsilon}{2} |||\mathbf{u}_h|||^2 + \frac{1}{2\epsilon} \|\eta \mathbf{v}_{p_h}\|^2_{1,\Omega,\mu} + \frac{C_I}{2\epsilon} \|\eta \mathbf{v}_{p_h}\|^2_{1,\Omega,\mu} \\ &\leq \frac{\epsilon}{2} |||\mathbf{u}_h|||^2 + \frac{(1 + C_I) C^2_{p1} \eta^2}{2\epsilon} \|p_h\|^2_{0,\Omega^+,\mu}. \qquad (24)\end{aligned}$$

Using (11), (22), (24) and (7) we obtain

$$\begin{aligned}
&\mathcal{B}_h[(\mathbf{u}_h, p_h), (\mathbf{v}_h, q_h)] + c_h(p_h, q_h) + s_h(p_h, q_h) \\
&\quad \geq C_a |||\mathbf{u}_h|||^2 - \frac{\epsilon}{2} |||\mathbf{u}_h|||^2 - \frac{(1 + C_I) C_{p1}^2 \eta^2}{2\epsilon} \|p_h\|_{0,\Omega^+,\mu}^2 + C_{p2} \|p_h\|_{0,\Omega^+,\mu}^2 \\
&\quad \geq (C_a - \frac{\epsilon}{2}) |||\mathbf{u}_h|||^2 + (C_{p2} - \frac{(1 + C_I) C_{p1}^2 \eta^2}{2\epsilon}) \|p_h\|_{0,\Omega^+,\mu}^2 \geq C_s \|(\mathbf{u}_h, p_h)\|_{\Omega^+}^2,
\end{aligned}$$

and, dividing by $\|(\mathbf{v}_h, q_h)\|_{\Omega^+}$, we have

$$\begin{aligned}
&\frac{\mathcal{B}_h[(\mathbf{u}_h, p_h), (\mathbf{v}_h, q_h)] + c_h(p_h, q_h) + s_h(p_h, q_h)}{\|(\mathbf{v}_h, q_h)\|_{\Omega^+}} \\
&\quad \geq \frac{\mathcal{B}_h[(\mathbf{u}_h, p_h), (\mathbf{v}_h, q_h)] + c_h(p_h, q_h) + s_h(p_h, q_h)}{\|(\mathbf{u}_h, p_h)\|_{\Omega^+}} \geq C_s \|(\mathbf{u}_h, p_h)\|_{\Omega^+}.
\end{aligned}$$

The thesis (10) of the theorem holds by choosing ϵ and η such that

$$\epsilon < 2C_a \quad \text{and} \quad \eta < \sqrt{\frac{2C_{p2}\epsilon}{(1 + C_I) C_{p1}^2}}.$$

□

3.2 Error analysis

We start from the consistency of the scheme, which will be useful for the derivation of the error estimate. For its derivation we follow [16] and [3].

Lemma 4 *Let* $(\mathbf{u}_h, p_h)$ *be the solution of the finite element formulation* (2) *and* $(\mathbf{u}, p) \in [H^2(\Omega_1 \cup \Omega_2)]^2 \times H^1(\Omega_1 \cup \Omega_2)$ *be the weak solution of* (1)*. Then the finite element formulation* (2) *fulfills the following consistency relation,*

$$\mathcal{B}_h[(\mathbf{u} - \mathbf{u}_h, p - p_h), (\mathbf{v}_h, q_h)] = c_h(p_h, q_h) + s_h(p_h, q_h), \forall (\mathbf{v}_h, q_h) \in V_h \times Q_h. \quad (25)$$

Proof The property follows by observing that the exact solution $(\mathbf{u}, p)$ satisfies

$$\mathcal{B}_h[(\mathbf{u}, p), (\mathbf{v}_h, q_h)] = (\mathbf{f}, \mathbf{v}_h)_\Omega, \forall (\mathbf{v}_h, q_h) \in V_h \times Q_h, \quad (26)$$

and then subtracting (2) to (26). □

We now analyze the approximation properties of the proposed finite element space, using the interpolation operator defined in [17]. As shown in [17], it enjoys the following approximation and stability properties:

Lemma 5 *The interpolation operator defined as in [17], namely* $R_h^* : H^s(\Omega) \to V_{h,0}$, *with* $s = 2$ *for the velocities and* $s = 1$ *for the pressure, is such that*

$$\|(\mathbf{v} - R_h^*\mathbf{v},\, p - R_h^* p)\|_{\Omega^+}^2 \leq h^2 \left(C_u \|\mu_{max}^{1/2}\mathbf{v}\|_{2,\Omega}^2 + C_p \|p\|_{1,\Omega^+,\mu}^2 \right)$$
$$(\textit{approximation}), \tag{27}$$
$$\|R_h^* w\|_{r,\Omega} \leq C \|w\|_{s,\Omega},\ \ 0 \leq r \leq \min(1, s),\ \ \forall w \in H^s(\Omega)$$
$$(\textit{stability}). \tag{28}$$

Starting from these results, we prove the following theorem.

Theorem 2 *The following error estimate holds true*

$$\|(\mathbf{u} - \mathbf{u}_h,\, p - p_h)\|_{\Omega^+} \leq Ch \left(\|\mu_{max}^{1/2}\mathbf{u}\|_{2,\Omega} + \|p\|_{1,\Omega^+,\mu} \right). \tag{29}$$

Proof .We have

$$\|(\mathbf{u} - \mathbf{u}_h,\, p - p_h)\|_{\Omega^+} \leq \|(\mathbf{u} - R_h^*\mathbf{u},\, p - R_h^* p)\|_{\Omega^+} + \|(R_h^*\mathbf{u} - \mathbf{u}_h,\, R_h^* p - p_h)\|_{\Omega^+}.$$

The first term can be estimated using the interpolation error estimate (27) directly,

$$\|(\mathbf{u} - R_h^*\mathbf{u},\, p - R_h^* p)\|_{\Omega^+} \leq Ch \left(\|\mu_{max}^{1/2}\mathbf{u}\|_{2,\Omega} + \|p\|_{1,\Omega^+,\mu} \right).$$

To estimate the second term we use the *inf-sup* condition (10), to get

$$\|(R_h^*\mathbf{u} - \mathbf{u}_h,\, R_h^* p - p_h)\|_{\Omega^+} \leq \sup_{\mathbf{v}_h, q_h \neq 0} C_s^{-1} (\mathcal{B}_h[(R_h^*\mathbf{u} - \mathbf{u}_h,\, R_h^* p - p_h),\, (\mathbf{v}_h, q_h)]$$
$$+ c_h(R_h^* p - p_h, q_h) + s_h(R_h^* p - p_h, q_h))/\|(\mathbf{v}_h, q_h)\|_{\Omega^+}.$$

Adding and subtracting the exact solutions $\mathbf{u}$ and p to $\mathcal{B}_h$ and using the consistency relation for the finite element formulation (25), we get

$$\|(R_h^*\mathbf{u} - \mathbf{u}_h,\, R_h^* p - p_h)\|_{\Omega^+} \leq \sup_{\mathbf{v}_h, q_h \neq 0} C_s^{-1} (\mathcal{B}_h[(\mathbf{u} - R_h^*\mathbf{u},\, p - R_h^* p),\, (\mathbf{v}_h, q_h)]$$
$$+ c_h(R_h^* p, q_h) + s_h(R_h^* p, q_h))/\|(\mathbf{v}_h, q_h)\|_{\Omega^+}.$$

Since the stabilization terms are symmetric we can use the Cauchy–Schwarz inequality followed by the continuity property (13) to obtain

$$c_h(R_h^* p, q_h) \leq c_h(R_h^* p, R_h^* p)^{1/2} c_h(q_h, q_h)^{1/2} \leq c_h(R_h^* p, R_h^* p)^{1/2} \|(\mathbf{v}_h, q_h)\|,$$

$$s_h(R_h^* p, q_h) \leq s_h(R_h^* p, R_h^* p)^{1/2} s_h(q_h, q_h)^{1/2} \leq s_h(R_h^* p, R_h^* p)^{1/2} \|(\mathbf{v}_h, q_h)\|.$$

Finally, by using the continuity of $\mathcal{B}_h[(\cdot,\cdot),(\cdot,\cdot)]$, (16), it follows that

$$\|(R_h^*\mathbf{u}-\mathbf{u}_h,\, R_h^*p-p_h)\|_{\Omega^+} \le C\Big(\|(\mathbf{u}-R_h^*\mathbf{u},\, p-R_h^*p)\|_{\Omega^+} + c_h(R_h^*p,\, R_h^*p)^{1/2} + s_h(R_h^*p,\, R_h^*p)^{1/2}\Big).$$

The first term is estimated using the interpolation error estimate (27). Then we use the definition of the stabilization terms and the stability properties of the interpolation operator (27) to obtain

$$c_h(R_h^*p,\, R_h^*p) \le Ch^2 \sum_{i=1}^{2} \|p_i\|^2_{1,\Omega_i^+,\mu}, \qquad s_h(R_h^*p,\, R_h^*p) \le Ch^2 \sum_{i=1}^{2} \|p_i\|^2_{1,\Omega_i^+,\mu}.$$

The thesis follows by combining the previous estimates. □

3.3 Conditioning of the Schur complement matrix

We are now interested in analyzing the conditioning of the system and in particular we focus on the Schur complement matrix. The forthcoming results will enable us to solve the discrete problem using the classical methods for saddle point problems like the Uzawa method [14]. Problem (2) can be written in algebraic form as

$$\begin{bmatrix} A & B^T \\ -B & S \end{bmatrix} \begin{bmatrix} u \\ p \end{bmatrix} = \begin{bmatrix} f_u \\ f_p \end{bmatrix}$$

where blocks are related to the bilinear forms, namely

$$a_h(\mathbf{u}_h, \mathbf{v}_h) = (\mathbf{v}_h, A\mathbf{u}_h), \quad b_h(\mathbf{u}_h, q_h) = (q_h, B\mathbf{u}_h)$$

while for the stabilization terms we have $S = S_1 + S_2$ where

$$c_h(p_h, q_h) = (q_h, S_1 p_h), \quad s_h(p_h, q_h) = (q_h, S_2 p_h).$$

The Schur complement $\mathcal{C}$ is defined as

$$\mathcal{C} = BA^{-1}B^T + S.$$

From (2), we define the following bilinear form,

$$\mathcal{L}_h\left[(\mathbf{u}_h, p_h), (\mathbf{v}_h, q_h)\right] = a_h(\mathbf{u}_h, \mathbf{v}_h) + b_h(\mathbf{v}_h, p_h) - b_h(\mathbf{u}_h, q_h) + c_h(p_h, q_h) + s_h(p_h, q_h). \tag{30}$$

and state the following assumptions:

Assumption A4 There exist positive numbers $C_a, C_b, C_{s1}, C_{s2}, C_B, \underline{\gamma}, \bar{\gamma}$, independent of $\mathbf{u}_h, \mathbf{v}_h, p_h, q_h$ such that

$$C_a |||\mathbf{v}_h|||^2 \leq a_h(\mathbf{v}_h, \mathbf{v}_h), \tag{31}$$

$$C_b(1+C)\|p_h\|_{0,\Omega^+,\mu} |||\mathbf{v}_h||| \geq b_h(\mathbf{v}_h, p_h), \tag{32}$$

$$C_{s1}\|p_h\|_{0,\Omega^+,\mu}\|q_h\|_{0,\Omega^+,\mu} \geq c_h(p_h, q_h), \tag{33}$$

$$C_{s2}\|p_h\|_{0,\Omega^+,\mu}\|q_h\|_{0,\Omega^+,\mu} \geq s_h(p_h, q_h), \tag{34}$$

$$C_B \|(\mathbf{u}_h, p_h)\|_{\Omega^+}\|(\mathbf{v}_h, q_h)\|_{\Omega^+} \geq \mathcal{B}_h[(\mathbf{u}_h, p_h), (\mathbf{v}_h, q_h)], \tag{35}$$

$$\underline{\gamma}\|(\mathbf{u}_h, p_h)\|_{\Omega^+} \leq \sup_{\mathbf{v}_h, q_h \neq 0} \frac{\mathcal{L}_h[(\mathbf{u}_h, p_h), (\mathbf{v}_h, q_h)]}{\|(\mathbf{v}_h, q_h)\|_{\Omega^+}}, \tag{36}$$

$$\bar{\gamma}\|(\mathbf{u}_h, p_h)\|_{\Omega^+} \geq \sup_{\mathbf{v}_h, q_h \neq 0} \frac{\mathcal{L}_h[(\mathbf{u}_h, p_h), (\mathbf{v}_h, q_h)]}{\|(\mathbf{v}_h, q_h)\|_{\Omega^+}}. \tag{37}$$

Analogously, there exist $\bar{\gamma}' \leq \bar{\gamma}$ such that

$$\bar{\gamma}'\|(\mathbf{u}_h, p_h)\|_{\Omega^+} \geq \sup_{\mathbf{v}_h, q_h \neq 0} \frac{b_h(\mathbf{u}_h, q_h) - c_h(p_h, q_h) - s_h(p_h, q_h)}{\|q\|_{0,\Omega^+,\mu}}. \tag{38}$$

We remark that the existence of $\bar{\gamma}'$ follows from (37) with $\bar{\gamma}' = \bar{\gamma}$. However, we can consider the case in which a better estimate of $\bar{\gamma}'$ may be available. Inequalities (31), (32), (33), (34) and (35) correspond to results of Lemma 1, and (36) is the thesis of Theorem 1. The equivalence of discrete norms (7) has been used in (13) to obtain (32). Inequality (37) follows from assumptions (33), (34) and (35).

Theorem 3 *Under assumption A4, the eigenvalues of $\mathcal{C}$ are localized as follows:*

$$\lambda_n(\mathcal{C}) \in \left\{ z \in \mathbb{C} : \underline{\gamma} \leq |z| \leq \bar{\gamma}' \sqrt{1 + \left(\frac{C_b(1+C)}{C_a}\right)^2} \right\}. \tag{39}$$

Proof To prove (39), we follow the general framework proposed in [11]. For each $p_h \in Q_h$, let $\tilde{\mathbf{u}}_h \in V_h$ be defined by

$$a_h(\tilde{\mathbf{u}}_h, \mathbf{v}_h) + b_h(\mathbf{v}_h, p_h) = 0 \quad \forall \mathbf{v}_h \in V, \quad \text{that is,} \quad \tilde{\mathbf{u}}_h = -A^{-1}B^T p_h. \tag{40}$$

Taking $\mathbf{u}_h = \tilde{\mathbf{u}}_h$ in (30), makes $\mathcal{L}_h[(\mathbf{u}_h, p_h), (\mathbf{v}_h, q_h)] = c_h(p_h, q_h) + s_h(p_h, q_h) - b_h(\mathbf{u}_h, q_h) = (q_h, \mathcal{C}p_h)$ independent of $\mathbf{v}_h$; hence, using (36) and (38),

$$\underline{\gamma}\|(\tilde{\mathbf{u}}_h, p_h)\|_{\Omega^+} \leq \sup_{\mathbf{v}_h, q_h \neq 0} \frac{(q_h, \mathcal{C}p_h)}{\|(\mathbf{v}_h, q_h)\|_{\Omega^+}} \leq \sup_{q_h \neq 0} \frac{(q_h, \mathcal{C}p_h)}{\|q_h\|_{0,\Omega^+,\mu}} \leq \bar{\gamma}'\|(\tilde{\mathbf{u}}_h, p_h)\|_{\Omega^+}. \tag{41}$$

From (40), (31) and (32) we have,

$$C_a |||\tilde{\mathbf{u}}_h|||^2 \leq a_h(\tilde{\mathbf{u}}_h, \tilde{\mathbf{u}}_h) = -b_h(\tilde{\mathbf{u}}_h, p_h) \leq C_b(1+C)\|p_h\|_{0,\Omega^+,\mu} |||\tilde{\mathbf{u}}_h|||,$$

so that $|||\tilde{\mathbf{u}}_h||| \leq \frac{C_b}{C_a}\|p_h\|_{\Omega^+}$, yielding the following estimate,

$$\|p_h\|_{0,\Omega^+,\mu} \leq \|(\tilde{\mathbf{u}}_h, p_h)\|_{\Omega^+} \leq \sqrt{1+\left(\frac{C_b(1+C)}{C_a}\right)^2}\|p_h\|_{0,\Omega^+,\mu}$$

and Eq. (41) becomes

$$\underline{\gamma}\|p_h\|_{0,\Omega^+,\mu} \leq \sup_{q_h\neq 0}\frac{(q_h, \mathcal{C}p_h)}{\|q_h\|_{0,\Omega^+,\mu}} \leq \bar{\gamma}'\sqrt{1+\left(\frac{C_b(1+C)}{C_a}\right)^2}\|p_h\|_{0,\Omega^+,\mu}.$$

□

4 Numerical results

We analyse the order of convergence of two variants of the proposed method compared with two reference methods and we investigate how Brezzi–Pitkaranta stabilization improves the conditioning of the algebraic problem.

4.1 Comparison of different variants of methods

The previous analysis is valid for those choices of finite element spaces and stabilization terms for which the *inf-sup* condition is guaranteed on the restricted sub-domains. The stabilization on the *extended cut region* makes the *inf-sup* condition to be globally satisfied. We analyze the numerical performances of the following combination:

- $\mathbb{P}^1_b - \mathbb{P}^1$ elements with Brezzi–Pitkaranta stabilization on the cut region. We notice that, since the *inf-sup* condition is satisfied because of the bubble stabilization, we do not need the additional term $c_h(p_h, q_h)$.
- $\mathbb{P}^1 - \mathbb{P}^1$ with Brezzi–Pitkaranta stabilization on all the domain, i.e. both $c_h(p_h, q_h)$ and $s_h(p_h, q_h)$ are active.

These two choices will be compared with two *reference methods*. The first one employs $\mathbb{P}^1_b - \mathbb{P}^1$ elements without any additional stabilization in the *extended cut region* ($s_h(p_h, q_h) = 0$). This is the method for which we observed instabilities in the pressure approximation, as hown in Fig. 1. The second one has been proposed by Burman–Becker–Hansbo [3] and it consists in choosing $\mathbb{P}^1 - \mathbb{P}^0$ elements with a stabilization based on the jump of the pressure along the edges of the mesh, so we define:

$$c_h(p_h, q_h) + s(p_h, q_h) := \sum_{F\in\mathcal{F}_1}\int_F \frac{\gamma_p}{\mu_1}h_F[\![p_{h,1}]\!][\![q_{h,1}]\!]ds + \sum_{F\in\mathcal{F}_2}\int_F \frac{\gamma_p}{\mu_2}h_F[\![p_{h,2}]\!][\![q_{h,2}]\!]ds, \tag{42}$$

where $\mathcal{F}_i$ denotes the set of interior faces of $\mathcal{T}^+_{h,i}$.

From the standpoint of accuracy, the considered methods are substantially equivalent. Indeed, they all satisfy the following theoretical estimate [12,20]:

$$\|\mathbf{u} - \mathbf{u}_h\|_{1,\Omega,\mu} + \|p - p_h\|_{0,\Omega^+,\mu} \leq Ch(\|\mathbf{u}\|_{2,\Omega} + \|p\|_{1,\Omega}). \tag{43}$$

In what follows we will show that the performance of all methods is coherent to the theory, but appreciable differences may appear in the magnitude of the error.

A strong point in favor of the Brezzi–Pitkaranta stabilization is that it is easy to implement, that is it keeps to a minimum the effort needed to introduce the stabilization term in a pre-existing finite element code. Moreover, it can be easily used in a parallel context. In contrast, the assembling of a stabilization term that needs integration on the edges of the elements, such as the Burman–Becker and Hansbo stabilization, usually requires to access information about the adjacent elements to each edge, which increases the communication between processors.

4.2 Test cases and results

The numerical tests have been implemented in the C++ finite element library `LifeV` (www.lifev.org), developed by the collaboration between four institutions: École Polytechnique Fédérale de Lausanne (CMCS), Politecnico di Milano (MOX), INRIA (REO, ESTIME) and Emory University.

We solve the saddle point problems in the domain $\Omega = [0, 1]^2$ crossed by the interface $\Gamma = \{x, y | (x - x_c)^2 + (y - y_c)^2 = a^2\}$. We set $a = 0.25$ and $x_c = y_c = 0.5$. Let us define $\Omega_1 = \{x, y | (x - x_c)^2 + (y - y_c)^2 < a^2\}$ the internal part of the domain with respect to the orientation of the normal of Γ, and Ω_2 is the external part. We set $\gamma_s = 1$ and the penalty parameters $\gamma_p = \gamma_u = 10$. The determination of these parameters is fairly heuristic. This is one of the major drawbacks of using penalty methods for pressure stabilization and to enforce interface conditions. The selected values have been tuned on the simple test case 1 described below, aiming to obtain a stable numerical solution that is not prerturbed by the consistency error due to pressure stabilization. These values have been then kept constant for all the other numerical experiments. The fact that they fit to all test cases suggests that they fall in the range where stability and accuracy criteria are simultaneously satisfied.

We consider three different test cases. In the first two tests there is no variation in the parameters of the problem between the two sides of the interface. The surface Γ is then an *artificial* interface, however the additional XFEM degrees of freedom and the weak imposition of the conditions across the surface can produce extra numerical errors in the region near the interface. We discuss in details the convergence analysis for the error on the velocity and pressure solution.

Test 1: Poiseuille's flow We start from the Poiseuille's flow in the domain Ω crossed by Γ, for the verification of the numerical solver. We remind that in a Poiseuille's flow, the velocity profile is parabolic for the horizontal component and null for the vertical one. The gradient of the pressure is linear. As we can see in Fig. 5, the numerical results are coherent with the theoretical estimates (43). The error constant of the stabilized $\mathbb{P}^1 - \mathbb{P}^0$ scheme is slightly larger than in the other cases. This behavior can

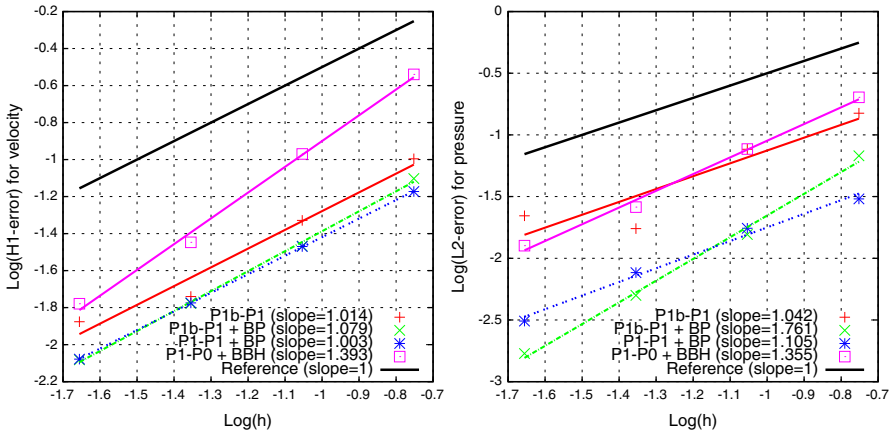

(a) H^1-norm error for velocity **(b)** L^2-norm error for pressure

Fig. 5 Convergence analysis for test 1

be explained observing that this method is the only one based on piecewise constant pressure elements, to approximate a linear pressure field.

Test 2: An artificial interface in an incompressible medium We analyse the case of an artificial interface in an incompressible fluid with constant material properties over the entire domain as proposed in [3] and [17]. For problem (1), the following continuous analytical solution is available,

$$\mathbf{u}(x, y) = \left[20xy^3; 5x^4 - 5y^4\right], \quad p(x, y) = 60x^2y - 20y^3 - 5,$$

and is obtained by setting the right hand side $\mathbf{f} = 0$. We observe that the velocity approximation error is very similar for the four considered methods. For the approximation of the pressure, methods based on the Brezzi–Pitkaranta stabilization perform slightly better that the others (Fig. 6).

Test 3: An elastic interface problem After these preliminary tests, we analyze a problem with heterogeneous coefficients [3]. This is an incompressible linear elastic problem that can be reinterpreted as a Stokes flow with suitable forcing terms. Let Ω be the unit square $[0, 1]^2$ and Ω_1 be the circle of radius $a = 0.25$ centered in $b = x_c = y_c = 0.5$, as defined above. We set $E_1 = E_2 = 1$, $\nu_2 = 0.25$ and $\nu_1 = 0.49$. Coefficients μ_i are defined as follows: $\mu_i = E_i/(2(1+\nu_i))$, $\lambda_i = E_i\nu_i/[(1+\nu_i)(1-2\nu_i)]$. Using polar coordinates, where $r = \sqrt{(x-b)^2 + (y-b)^2}$, the analytical solution for velocity and pressure is given by the following expressions, for $\nu_1 \neq 0.5$:

$$u_r(r, \theta) = \begin{cases} c_1 r & \text{in } \Omega_1 \\ \left(r - \frac{b^2}{r}\right)c_2 + \frac{b^2}{r} & \text{in } \Omega_2 \end{cases}$$

$$u_\theta(r, \theta) = 0$$

$$p(r, \theta) = \begin{cases} -2c_1\lambda_1 & \text{in } \Omega_1 \\ -2c_2\lambda_2 & \text{in } \Omega_2 \end{cases}$$

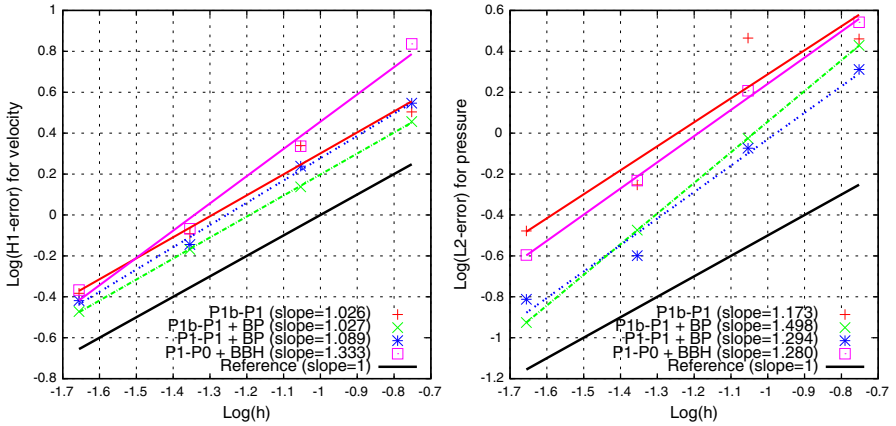

(a) H^1-norm error for velocity **(b)** L^2-norm error for pressure

Fig. 6 Convergence analysis for test 2

$$c_1 = \left(1 - \frac{b^2}{a^2}\right) c_2 + \frac{b^2}{a^2}$$
$$c_2 = \frac{(\lambda_1 + \mu_1 + \mu_2) b^2}{(\lambda_2 + \mu_2) a^2 + (\lambda_1 + \mu_1)(b^2 - a^2) + \mu_2 b^2},$$

which exactly satisfy the interface conditions of (1). The solution of this test case, calculated using $\mathbb{P}^1_b - \mathbb{P}^1$ elements, is shown in Fig. 1. The momentum and mass conservation equation of (1) are satisfied, provided that the right hand sides $\mathbf{f}$ and g are chosen for the momentum and continuity equations, respectively,

$$\mathbf{f} = 0, \qquad g = -\frac{p_i}{\lambda_i} \quad \text{in} \quad \Omega_i.$$

We notice that the variation on the Poisson coefficient produces a kink in the radial velocity profile and a strong discontinuity in the pressure solution (Fig. 1a, b). Strictly speaking, p can be interpreted as the pressure only in the incompressible case (Stokes problem), but we shall omit this distinction. Similarly to the previous results, performances of the methods are quite similar concerning the velocity approximation. When the pressure field is discontinuous, Fig. 7 shows that resorting to a stabilization method on the cut region is recommended. However, the best performances are obtained when pressure stabilization is adopted on the entire domain, combined with either $\mathbb{P}^1 - \mathbb{P}^0$ or $\mathbb{P}^1 - \mathbb{P}^1$ elements. Finally, we are interested in studying the behavior of the scheme for two different choices of weights k_i. In Fig. 8, we collect the results of the test discussed above, performed using the weights defined in [16], which do not account for the heterogeneity of viscosity. Comparing the results reported in Figs. 7 and 8, we do not observe a significant difference. We remark that the computational cost of these weights is very similar and we conclude that both the choices are suitable to solve a problem with a mild heterogeneity between coefficients.

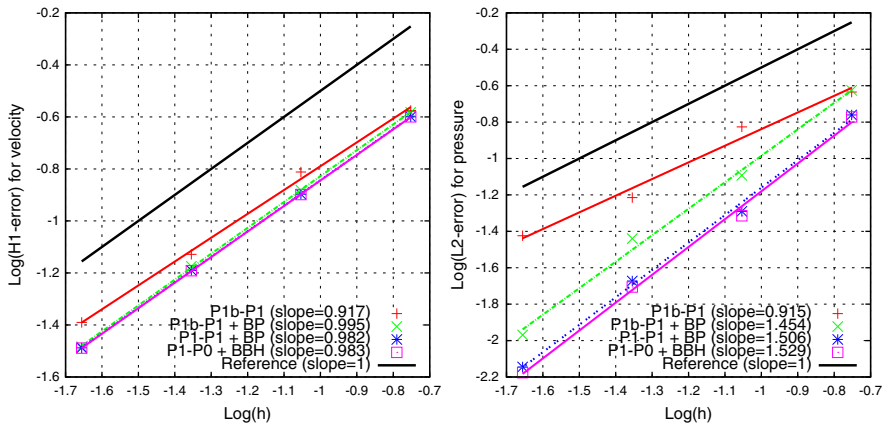

(a) H^1-norm error for velocity **(b)** L^2-norm error for pressure

Fig. 7 Convergence analysis for test 3, using the averaging weights defined in (3)

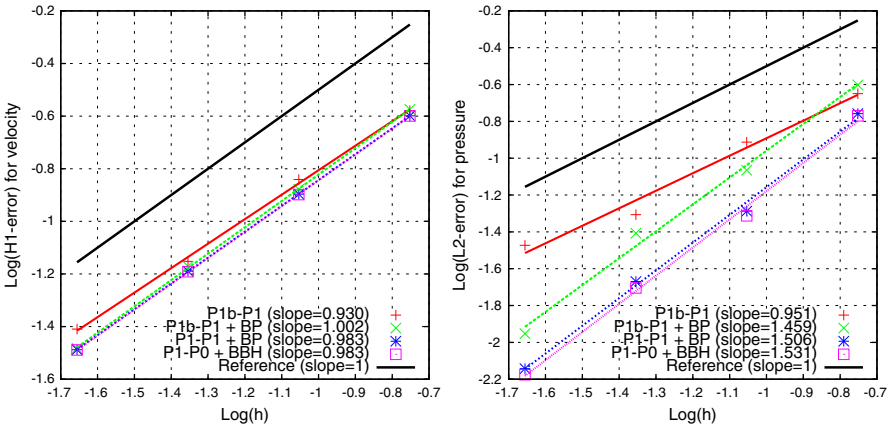

(a) H^1-norm error for velocity **(b)** L^2-norm error for pressure

Fig. 8 Convergence analysis for test 3, using the averaging weights defined in [16]

We finally observe that for the analysis of the numerical experiments we have used the standard H^1 and L^2 norms for velocity and pressure respectively, while the theoretical error estimate of the scheme we have analyzed is provided for $\|(\mathbf{u}-\mathbf{u}_h,\, p-p_h)\|_{\Omega^+}$. We claim that the norms considered for the numerical tests are the dominating terms of this more general error indicator. This is confirmed by Fig. 9, where we show $\|[\![\mathbf{u}_h]\!]\|_{1/2,h,\Gamma}$. This term is a part of $\|(\mathbf{u}-\mathbf{u}_h,\, p-p_h)\|_{\Omega^+}$ and it scales as $h^{3/2}$, in agreement with the expected theoretical estimate. We notice that its magnitude is significantly smaller than the one of the velocity H^1 norm.

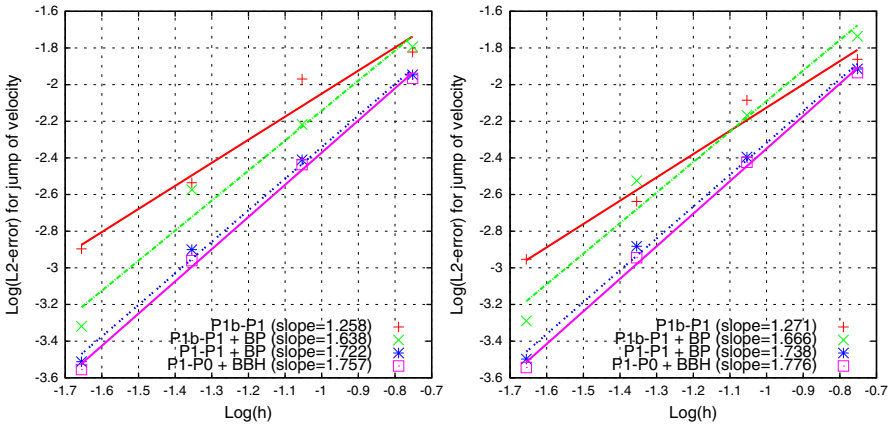

(a) Dolbow weights **(b)** Standard weights

Fig. 9 L^2-norm error for the jump of velocity across the interface

4.3 Problem conditioning

As we already pointed out, the Nitsche-XFEM method allows for using meshes independent of the position of Γ, but instabilities in the cut region depend on how the interface crosses the elements. For this reason, we study the conditioning of the pressure Schur complement matrix $\mathcal{C}$ for the third test case previously described and we use the $\mathbb{P}^1-\mathbb{P}^1$ elements with Brezzi–Pitkaranta stabilization. By increasing the radius of the circular interface Γ, see Fig. 1, we modify the intersections between the mesh and the interface. According to Theorem 3, we expect the condition number of the stabilized method is not affected by the geometry of the interface. The calculation of the condition number is done following [18].

In Table 1, we collect the obtained results. First of all, we observe that the conditioning of matrix $\mathcal{C}$ is almost constant when using $\mathbb{P}^1-\mathbb{P}^1$ elements with Brezzi–Pitkaranta stabilization on the whole domain, as expected from (39). The condition number is independent of how the interface cuts the mesh.

In addition, we calculate the minimum eigenvalue of the Schur complement matrix, preconditioned with the pressure mass matrix. When the pressure stabilization on the cut region is active, we use $\mathcal{M}_p^+$ defined as,

$$\left[\mathcal{M}_p^+\right]_{mn} = \sum_{i=1}^{2} \int_{\Omega_i^+} q_h^m q_h^n dx, \qquad q_h^m, q_h^n \in Q_h,$$

where we remark that the integrals of basis functions having support in a $K \in \mathcal{G}_h$ are computed on the entire element K. For the non stabilized case, the usual definition is applied,

$$\left[\mathcal{M}_p\right]_{mn} = \sum_{i=1}^{2} \int_{\Omega_i} q_h^m q_h^n dx, \qquad q_h^m, q_h^n \in Q_h.$$

Table 1 Conditioning of the preconditioned Schur complement $\mathcal{C}$ for small perturbations of the radius r of Ω_1 (top)

r	$\min\left\{\frac{\lvert K\cap\Omega_1\rvert}{\lvert K\cap\Omega_2\rvert}\right\}$	$\kappa(\mathcal{M}_p^{-1}\mathcal{C})$ $\mathbb{P}^1_{bubble}-\mathbb{P}^1$	$\kappa((\mathcal{M}_p^{+})^{-1}\mathcal{C})$ $\mathbb{P}^1-\mathbb{P}^1$ + BP stab.	$\kappa((\mathcal{M}_p^{+})^{-1}\mathcal{C})$ $\mathbb{P}^1_{bubble}-\mathbb{P}^1$ + BP stab.
0.250	0.31038	8.15×10^{2}	1.35×10^{3}	559.83
0.270	0.02990	8.27×10^{3}	1.36×10^{3}	654.35
0.280	3.35×10^{-4}	2.61×10^{7}	1.37×10^{3}	2.66×10^{3}
0.281	1.34×10^{-5}	2.18×10^{8}	1.37×10^{3}	9.14×10^{3}
r	$\min\left\{\frac{\lvert K\cap\Omega_1\rvert}{\lvert K\cap\Omega_2\rvert}\right\}$	$\min\{\lambda_i(\mathcal{M}_p^{-1}\mathcal{C})\}$ $\mathbb{P}^1_{bubble}-\mathbb{P}^1$	$\min\{\lambda_i((\mathcal{M}_p^{+})^{-1}\mathcal{C})\}$ $\mathbb{P}^1-\mathbb{P}^1$ + BP stab.	$\min\{\lambda_i((\mathcal{M}_p^{+})^{-1}\mathcal{C})\}$ $\mathbb{P}^1_{bubble}-\mathbb{P}^1$ + BP stab.
0.250	0.31038	−1.6434	0.486	0.2318
0.270	0.02990	−2.6736	0.4945	0.2316
0.280	3.35×10^{-4}	−4.3228	0.4939	0.1359
0.281	1.34×10^{-5}	−22.1581	0.4936	0.1235

Minumun eigenvalue of the preconditioned Schur complement $\mathcal{C}$ for small perturbations of the radius of Ω_1 (bottom)

The quantities $\min\{\lambda_i((\mathcal{M}_p^{+})^{-1}\mathcal{C})\}$ and $\min\{\lambda_i(\mathcal{M}_p^{-1}\mathcal{C})\}$ inform us about the *inf-sup* stability of the scheme, because they are directly proportional to the *inf-sup* constant [12]. The analysis is reported in Table 1. The fact that the minimum eigenvalue of $\min\{\lambda_i(\mathcal{M}_p^{-1}\mathcal{C})\}$ is nor positive, neither bounded from below when the size of cut elements decreases, confirms the lack of stability of the approximation method without pressure stabilization. Conversely, the Brezzi–Pitkaranta stabilization, applied on the cut region or on the whole domain, restores the desired positivity and boundedness property, almost uniformly with respect to the cut-element size.

5 Conclusions

This work arises from the observation that the approximation of saddle point problems with extended finite elements poses some stability issues. In particular, for the Stokes problem the approximation of the pressure may be locally unstable. Standard mixed finite element spaces combined with simple enrichment strategies lead to a satisfactory approximation method, provided that pressure stabilization is introduced into the scheme. The general framework of symmetric stabilization techniques is suitable to cure this kind of issues. In particular, we have shown that the Brezzi–Pitkaranta stabilization scheme is effective also in this new approximation context. The algebraic properties of the scheme are also analyzed, enabling the application of standard solvers, such as the Uzawa method.

Acknowledgments This project was supported by the ERC Advanced Grant N.227058 MATHCARD and by Politecnico di Milano through the grant "5/1000 Junior—Computational models for heterogeneous media" CUP D41J10000490001. The second and fourth authors also acknowledge the support of the Italian

MIUR through PRIN09 project n. 2009Y4RC3B 001. The authors would also like to thank Dr. Alessio Fumagalli and Dr. Antonio Cervone for many fruitful discussion on the implementation of the original code in `LifeV`.

References

1. Annavarapu, C., Hautefeuille, M., Dolbow, J.E.: A robust Nitsche's formulation for interface problems. Comput. Methods Appl. Mech. Eng. **225–228**, 44–54 (2012)
2. Ausas, R.F., Buscaglia, G.C., Idelsohn, S.R.: A new enrichment space for the treatment of discontinuous pressures in multi-fluid flows. Int. J. Numer. Methods Fluids **70**(7), 829–850 (2012)
3. Becker, R., Burman, E., Hansbo, P.: A Nitsche extended finite element method for incompressible elasticity with discontinuous modulus of elasticity. Comput. Methods Appl. Mech. Eng. **198**(41–44), 3352–3360 (2009)
4. Brenner, S.C., Scott, L.R.: The Mathematical Theory of Finite Element Methods, Springer-Verlag, New York (2008)
5. Brezzi, F., Fortin, M.: Mixed and hybrid finite element methods. Springer Series in Computational Mathematics, vol. 15. Springer, New York (1991)
6. Brezzi, F., Pitkäranta, J.: On the stabilization of finite element approximations of the Stokes equations. In: Efficient Solutions of Elliptic Systems (Kiel, 1984). Notes Numer. Fluid Mech., vol. 10, pp. 11–19. Vieweg, Braunschweig (1984)
7. Burman, E.: Ghost penalty [la pénalisation fantôme]. Comptes Rendus Mathematique **348**(21–22), 1217–1220 (2010)
8. Burman, E., Hansbo, P.: Fictitious domain methods using cut elements: III. A stabilized Nitsche method for Stokes' problem. Technical Report 2011:06, School of Engineering, Jönköping University, JTH, Mechanical Engineering (2011)
9. Burman, E., Hansbo, P.: Fictitious domain finite element methods using cut elements: II. a stabilized Nitsche method. Appl. Numer. Math. **62**(4), 328–341 (2012)
10. Buscaglia, G.C., Agouzal, A.: Interpolation estimate for a finite-element space with embedded discontinuities. IMA J. Numer. Anal. **32**(2), 672–686 (2012)
11. D'Angelo, C., Zunino, P.: Robust numerical approximation of coupled Stokes' and Darcy's flows applied to vascular hemodynamics and biochemical transport. ESAIM: Math. Model. Numer. Anal. **45**(3), 447–476 (2011)
12. Ern, A., Guermond, J.: Theory and practice of finite elements. Applied Mathematical Sciences, vol. 159. Springer, New York (2004)
13. Fries, T.-P., Belytschko, T.: The extended/generalized finite element method: an overview of the method and its applications. Int. J. Numer. Methods Eng. **84**(3), 253–304 (2010)
14. Girault, V., Raviart, P.: Finite element methods for Navier-Stokes equations. Springer Series in Computational Mathematics, Theory and Algorithms, vol. 5. Springer, Berlin (1986)
15. Gross, S., Reusken, A.: Numerical methods for two-phase incompressible flows. Springer Series in Computational Mathematics, vol. 40. Springer, Berlin (2011)
16. Hansbo, A., Hansbo, P.: An unfitted finite element method, based on Nitsche's method, for elliptic interface problems. Comput. Methods Appl. Mech. Eng. **191**(47–48), 5537–5552 (2002)
17. Hansbo, P., Larson, M.G., Zahedi, S.: A cut finite element method for a Stokes interface problem. arXiv preprint arXiv:1205.5684 (2012)
18. Higham, N.J., Tisseur, F.: A block algorithm for matrix 1-norm estimation, with an application to 1-norm pseudospectra. SIAM J. Matrix Anal. Appl. **21**(4), 1185–1201 (2000)
19. Massing, A., Larson, M.G., Logg, A., Rognes, M.E.: A stabilized Nitsche fictitious domain method for the Stokes problem. arXiv preprint arXiv:1206.1933 (2012)
20. Quarteroni, A., Valli, A.: Numerical Approximation of Partial Differential Equations. Springer, Berlin (2008)
21. Reusken, A.: Analysis of an extended pressure finite element space for two-phase incompressible flows. Comput. Vis. Sci. **11**(4–6), 293–305 (2008)
22. Reusken, A., Esser, P.: Analysis of time discretization methods for stokes equations with a nonsmooth forcing term. Numerische Mathematik.179(3–4), 1–27 (2013)
23. Sauerland, H., Fries, T.-P.: The extended finite element method for two-phase and free-surface flows: a systematic study. J. Comput. Phys. **230**(9), 3369–3390 (2011)

24. Sousa, F.S., Ausas, R.F., Buscaglia, G.C.: Numerical assessment of stability of interface discontinuous finite element pressure spaces. Comput. Methods Appl. Mech. Eng. **245–246**, 63–74 (2012)
25. Zilian, A., Netuzhylov, H.: Hybridized enriched space-time finite element method for analysis of thin-walled structures immersed in generalized Newtonian fluids. Comput. Struct. **88**(21–22), 1265–1277 (2010)
26. Zunino, P.: Analysis of backward Euler/extended finite element discretization of parabolic problems with moving interfaces. Comput. Methods Appl. Mech. Eng. **258**, 152–165 (2013)
27. Zunino, P., Cattaneo, L., Colciago, C.M.: An unfitted interface penalty method for the numerical approximation of contrast problems. Appl. Numer. Math. **61**(10), 1059–1076 (2011)